

# European Urology

## A Ready To Use Web-Application Providing a Personalized Biopsy Schedule for Men With Low-Risk PCa Under Active Surveillance --Manuscript Draft--

<b>Manuscript Number:</b>	
<b>Article Type:</b>	Original Article
<b>Section/Category:</b>	Prostate Cancer (PRO)
<b>Keywords:</b>	Active Surveillance, Biopsies, Personalized Medicine, Prostate Cancer, Shared Decision Making
<b>Corresponding Author:</b>	Anirudh Tomer, M.Sc. Erasmus MC NETHERLANDS
<b>First Author:</b>	Anirudh Tomer, M.Sc.
<b>Order of Authors:</b>	Anirudh Tomer, M.Sc. Daan Nieboer, MSc Monique J Roobol, PhD Anders Bjartell, MD, PhD Ewout W Steyerberg, PhD Dimitris Rizopoulos, PhD
<b>Abstract:</b>	<p><b>Background:</b> Prostate cancer active surveillance (AS) patients undergo repeat biopsies. Active treatment is advised when biopsy Gleason grade group <math>\geq 2</math> (upgrading). Many patients never experience upgrading, yet undergo biopsies frequently. Personalized biopsy decisions based on upgrading-risk may reduce patient burden.</p> <p><b>Objective:</b> Develop a risk prediction model and web-application to assist patients/doctors in personalized biopsy decisions.</p> <p><b>Design, Setting, and Participants:</b> Model development: world's largest AS study PRIAS, 7813 patients, 1134 experienced upgrading; External validation: largest six cohorts of Movember Foundation's GAP3 database (<math>&gt;20,000</math> patients, 27 centers worldwide);</p> <p><b>Data:</b> repeat prostate-specific antigen (PSA) and biopsy Gleason grade group.</p> <p><b>Outcome Measurements, and Statistical Analysis:</b> A Bayesian joint model fitted to PRIAS dataset. This model was validated in GAP3 cohorts using risk prediction error, calibration, area under ROC (AUC). Model and personalized biopsy schedules based on predicted risks were implemented in a web-application.</p> <p><b>Results and Limitations:</b> Cause-specific cumulative upgrading-risk at year five of follow-up: 35% in PRIAS, at most 50% in GAP3 cohorts. PRIAS based model: PSA velocity was stronger predictor of upgrading (Hazard Ratio: 2.47, 95%CI: 1.93 - 2.99) than PSA value (Hazard Ratio: 0.99, 95%CI: 0.89 - 1.11). Validation: Moderate AUC (0.55 - 0.75) in PRIAS and GAP3 cohorts. Moderate prediction error (0.1 - 0.3) in GAP3 cohorts where impact of PSA value and velocity on upgrading-risk was similar to PRIAS, but large (0.3 - 0.45) otherwise. Recalibration of baseline risk required for external cohorts.</p> <p><b>Conclusions:</b> We successfully developed and validated a model for predicting upgrading-risk, and providing risk-based personalized biopsy decisions, in prostate cancer AS. The model made available via a web-application enables shared decision making of biopsy schedules by comparing fixed and personalized schedules on total biopsies and expected time delay in detecting upgrading.</p> <p><b>Patient Summary:</b> Personalized prostate biopsies are a novel alternative to fixed one-size-fits-all schedules. The underlying statistical models are made available through a user-friendly web-application and may help to reduce unnecessary prostate biopsies while maintaining cancer control.</p>
<b>Suggested Reviewers:</b>	
<b>Opposed Reviewers:</b>	

# A Ready To Use Web-Application Providing a Personalized Biopsy Schedule for Men With Low-Risk PCa Under Active Surveillance\*

Anirudh Tomer, MSc<sup>a,\*</sup>, Daan Nieboer, MSc<sup>b,c</sup>, Monique J. Roobol, PhD<sup>c</sup>, Anders Bjartell, MD, PhD<sup>d</sup>, Ewout W. Steyerberg, PhD<sup>b,e</sup>, Dimitris Rizopoulos, PhD<sup>a</sup>, Movember Foundation's Global Action Plan Prostate Cancer Active Surveillance (GAP3) consortium<sup>f</sup>

<sup>a</sup>*Department of Biostatistics, Erasmus University Medical Center, Rotterdam, the Netherlands*

<sup>b</sup>*Department of Public Health, Erasmus University Medical Center, Rotterdam, the Netherlands*

<sup>c</sup>*Department of Urology, Erasmus University Medical Center, Rotterdam, the Netherlands*

<sup>d</sup>*Department of Urology, Skåne University Hospital, Malmö, Sweden*

<sup>e</sup>*Department of Biomedical Data Sciences, Leiden University Medical Center, Leiden, the Netherlands*

<sup>f</sup>*The Movember Foundation's Global Action Plan Prostate Cancer Active Surveillance (GAP3) consortium members presented in Appendix A*

---

## Abstract

**Background:** Prostate cancer active surveillance (AS) patients undergo repeat biopsies. Active treatment is advised when biopsy Gleason grade group  $\geq 2$  (*upgrading*). Many patients never experience upgrading, yet undergo biopsies frequently. Personalized biopsy decisions based on upgrading-risk may

---

\*Word count: abstract (headings excluded) 300; Text 2488; Total 2788

\*Corresponding author (Anirudh Tomer): Erasmus MC, kamer flex Na-2823, PO Box 2040, 3000 CA Rotterdam, the Netherlands. Tel: +31 10 70 43393

*Email addresses:* [a.tomer@erasmusmc.nl](mailto:a.tomer@erasmusmc.nl) (Anirudh Tomer, MSc), [d.nieboer@erasmusmc.nl](mailto:d.nieboer@erasmusmc.nl) (Daan Nieboer, MSc), [m.roobol@erasmusmc.nl](mailto:m.roobol@erasmusmc.nl) (Monique J. Roobol, PhD), [anders.bjartell@med.lu.se](mailto:anders.bjartell@med.lu.se) (Anders Bjartell, MD, PhD), [e.w.steyerberg@lumc.nl](mailto:e.w.steyerberg@lumc.nl) (Ewout W. Steyerberg, PhD), [d.rizopoulos@erasmusmc.nl](mailto:d.rizopoulos@erasmusmc.nl) (Dimitris Rizopoulos, PhD)

reduce patient burden.

**Objective:** Develop a risk prediction model and web-application to assist patients/doctors in personalized biopsy decisions.

**Design, Setting, and Participants:** Model development: world's largest AS study PRIAS, 7813 patients, 1134 experienced upgrading; External validation: largest six cohorts of Movember Foundation's GAP3 database ( $> 20,000$  patients, 27 centers worldwide); Data: repeat prostate-specific antigen (PSA) and biopsy Gleason grade group.

**Outcome Measurements, and Statistical Analysis:** A Bayesian joint model fitted to PRIAS dataset. This model was validated in GAP3 cohorts using risk prediction error, calibration, area under ROC (AUC). Model and personalized biopsy schedules based on predicted risks were implemented in a web-application.

**Results and Limitations:** Cause-specific cumulative upgrading-risk at year five of follow-up: 35% in PRIAS, at most 50% in GAP3 cohorts. PRIAS based model: PSA velocity was stronger predictor of upgrading (Hazard Ratio: 2.47, 95%CI: 1.93–2.99) than PSA value (Hazard Ratio: 0.99, 95%CI: 0.89–1.11). Validation: Moderate AUC (0.55–0.75) in PRIAS and GAP3 cohorts. Moderate prediction error (0.1–0.3) in GAP3 cohorts where impact of PSA value and velocity on upgrading-risk was similar to PRIAS, but large (0.3–0.45) otherwise. Recalibration of baseline risk required for external cohorts.

**Conclusions:** We successfully developed and validated a model for predicting upgrading-risk, and providing risk-based personalized biopsy decisions, in prostate cancer AS. The model made available via a web-application enables shared decision making of biopsy schedules by comparing fixed and personalized schedules on total biopsies and expected time delay in detecting upgrading.

**Patient Summary:** Personalized prostate biopsies are a novel alternative to fixed one-size-fits-all schedules. The underlying statistical models are made available through a user-friendly web-application and may help to reduce unnecessary prostate biopsies while maintaining cancer control.

**Keywords:** Active Surveillance, Biopsies, Personalized Medicine, Prostate Cancer, Shared Decision Making

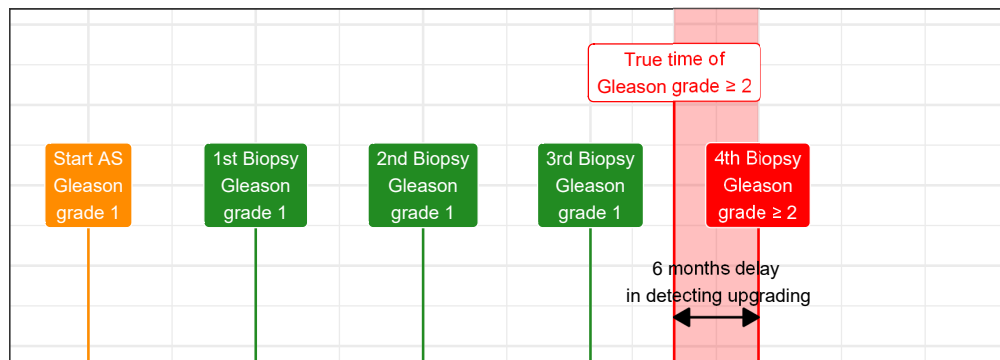
---

## 1. Introduction

Patients with low- and very low-risk screening-detected localized prostate cancer are usually recommended active surveillance (AS) instead of immediate radical treatment [1]. In AS, cancer progression is routinely monitored via prostate-specific antigen (PSA), digital rectal examination, and repeat biopsies. Among these, the strongest indicator of cancer-related outcomes is the biopsy Gleason grade group [2]. When it increases from group 1 (Gleason 3+3) to 2 (Gleason 3+4) or higher, called *upgrading* [3], patients are commonly advised curative treatment [4].

Usually, AS protocols schedule biopsies periodically. Consequently, up-

### A Biopsy every year



### B Biopsy every 2 years

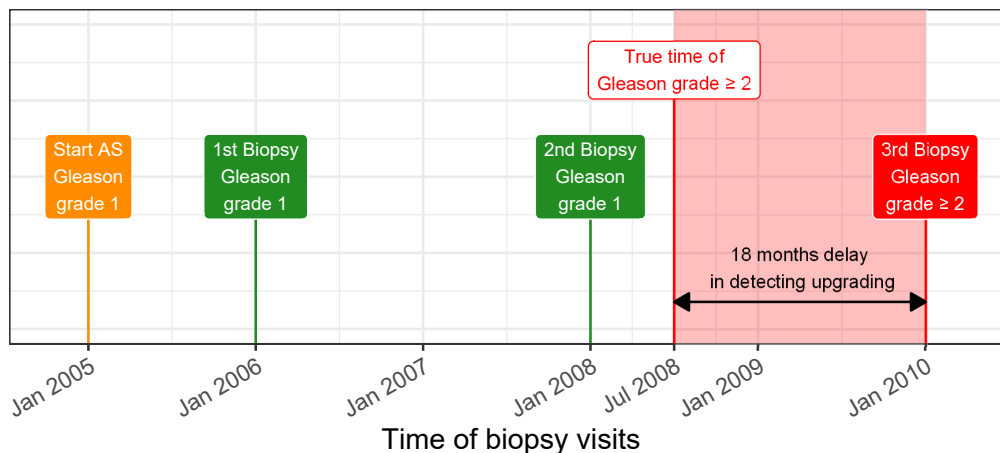


Figure 1: **Trade-off between the number of biopsies and time delay in detecting upgrading (Increase in Gleason grade group from 1 to 2 or higher):** The true time of upgrading for the patient in this figure is July 2008. When biopsies are scheduled annually (**Panel A**), upgrading is detected in January 2009 with a time delay of six months, and a total of four biopsies are scheduled. When biopsies are scheduled biennially (**Panel B**), upgrading is detected in January 2010 with a time delay of 18 months, and a total of three biopsies are scheduled. Since biopsies are conducted periodically, the time of upgrading is observed as an interval. For example, between Jan 2008–Jan 2009 in **Panel A** and between Jan 2008–Jan 2010 in **Panel B**. The phrase ‘Gleason grade group’ is shortened to ‘Gleason grade’ for brevity.

grading is always detected with a time delay (Figure 1). For detecting upgrading timely, many AS programs schedule fixed and frequent biopsies (e.g., annually) for all patients [5, 6]. However, this leads to unnecessary biopsies in slow/non-progressing patients. Biopsies are invasive, may be painful, and are prone to medical complications such as bleeding and septicemia[7]. Biopsy burden and patient non-compliance to frequent biopsies [8] have raised concerns regarding the optimal biopsy schedule [9, 10]. In this regard, in some cohorts, magnetic resonance imaging (MRI) is employed for targeted biopsies and to study its value for tumor monitoring. Although, due to currently limited AS data, MRI’s value is not clear. Others have proposed the option of scheduling biopsies infrequently (e.g., biennially) [9, 11]. However, due to differences in baseline upgrading-risk across cohorts [9], fixed biopsy schemes can still lead to many unnecessary biopsies. A promising alternative to fixed schedules are personalized biopsy schedules based on the patient-specific upgrading-risk (Figure 2).

The first challenge in creating personalized biopsy schedules is developing a statistical model to consolidate accumulated patient data (e.g., PSA, previous biopsy results) into predictions for upgrading-risk. Existing upgrading-risk [12, 13] calculators use only the latest PSA measurement of a patient. Comparatively, more information is captured by considering all repeatedly measured PSA, previous biopsy results, and baseline characteristics of a patient. To this end, a suitable model is the joint model for time-to-event and longitudinal data [14, 15, 16]. A joint model predicts upgrading-risk in a personalized manner. However, a subsequent challenge is translating predicted risks into clinical decisions. For example, a 10% upgrading-risk can

**A** Should a biopsy be conducted at current visit?

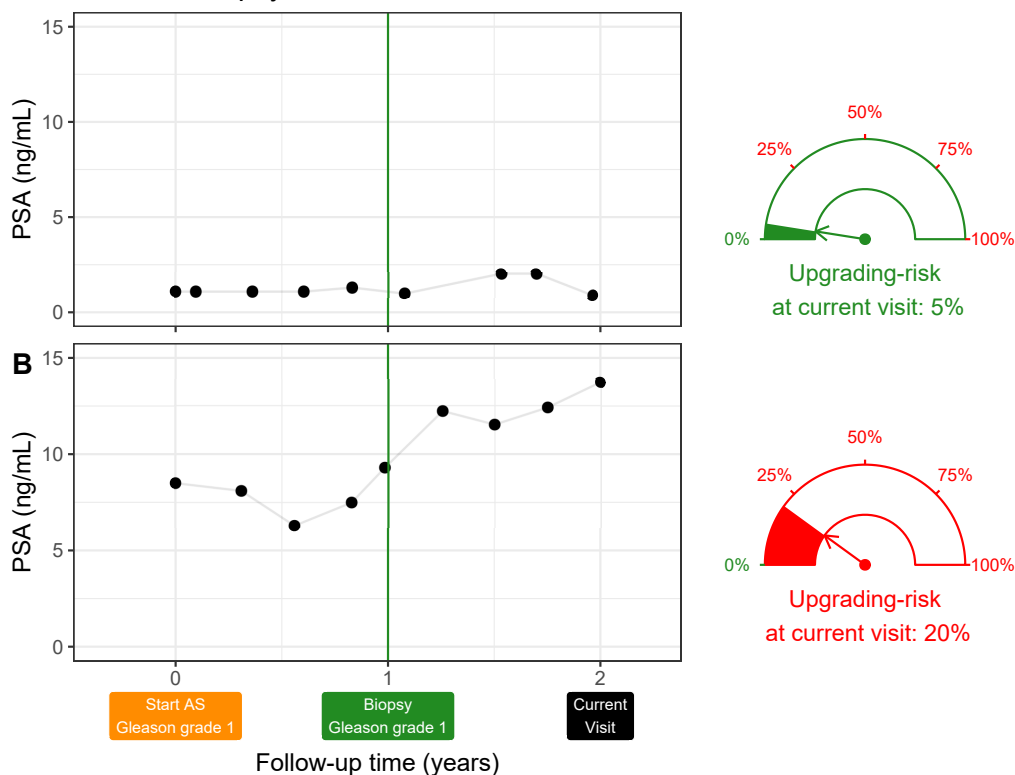


Figure 2: **Motivation for personalized upgrading-risk based decisions of biopsy:** Patient A (**Panel A**) and B (**Panel B**) had their latest biopsy at year one of follow-up (green vertical line). Patient A's prostate-specific antigen (PSA) profile remained stable until his current visit at year two, whereas patient B's profile has shown a rise. Consequently, patient B's upgrading-risk at the current visit (year two) is higher than that of patient A. This makes patient B a more suitable candidate for biopsy than Patient A. Risk estimates in this figure are only illustrative.

be perceived high/low depending upon the patient’s age. Patients may also weigh risks of upgrading with the potential *consequences* of another biopsy. Two such relevant consequences (Figure 1) are the timing and the total number of planned biopsies (burden), and the time delay in detecting upgrading (smaller is beneficial). The relative importance of these consequences can vary between the patients, and also within a patient over the follow-up period.

The goal of this work is two-fold. First, to develop a robust, generalizable model that gives reliable estimates for individual upgrading-risk in AS. Second, to utilize the predicted upgrading-risks to create personalized biopsy schedules. To facilitate shared decision making of biopsy schedules, we also intend to provide quantitative estimates of the aforementioned *consequences* of opting for a personalized versus the standard fixed schedule. For developing our model, we will use the world’s largest AS dataset PRIAS. Subsequently, we want to externally validate our model in the largest six AS cohorts from the Movember Foundation’s GAP3 database [17]. Last, we intend to implement our model and methodology in a web-application.

## 2. Patients and Methods

### 2.1. Study Cohort

For developing a statistical model to predict upgrading-risk, we used the world’s largest AS dataset, Prostate Cancer International Active Surveillance or PRIAS [4], dated April 2019 (Table 1). In PRIAS, PSA was measured quarterly for the first two years of follow-up and semiannually thereafter. Biopsies were scheduled at year one, four, seven, and ten of follow-up. Addi-



60 tional yearly biopsies were scheduled when PSA doubling time was between  
 61 zero and ten years.

62 We selected all 7813 patients who had Gleason grade group 1 at the time  
 63 of inclusion in PRIAS. Our primary event of interest is an increase in this  
 64 Gleason grade group observed upon repeat biopsy, called *upgrading* (1134 pa-  
 65 tients). Upgrading is a trigger for treatment advice in PRIAS. Also, 2250 pa-  
 66 tients were provided treatment based on their PSA, number of biopsy cores  
 67 with cancer, or anxiety/other reasons. Our reasons for focusing solely on  
 68 upgrading are, namely, upgrading is strongly associated with cancer-related  
 69 outcomes, and other treatment triggers vary between cohorts [5].

70 For model validation, we selected the following largest (by number of  
 71 repeated measurements) six cohorts from Movember Foundation’s GAP3  
 72 database version 3.1 [17]: University of California San Francisco AS (UCSF,  
 73 version 3.2), University of Toronto AS (Toronto), Johns Hopkins AS (Hop-  
 74 kins), Memorial Sloan Kettering Cancer Center AS (MSKCC), King’s College  
 75 London AS (KCL), and Michigan Urological Surgery Improvement Collabo-  
 76 rative AS (MUSIC). Only patients with a Gleason grade group 1 at the time  
 77 of inclusion in these cohorts were selected. Summary statistics are presented  
 78 in Supplementary A.2.

## 79 2.2. Statistical Model

80 For developing an upgrading-risk prediction model, the data we utilized  
 81 from the PRIAS cohort was patient age at inclusion in AS, longitudinally  
 82 measured PSA, timing of repeat biopsies and Gleason grades, and observed  
 83 time of upgrading. Analysis of this data required modeling the within-patient  
 84 correlation for PSA, the association between the Gleason grades and PSA

Table 1: **Summary of the PRIAS dataset as of April 2019.** The primary event of interest is upgrading, that is, increase in Gleason grade group from group 1 [2] to 2 or higher. IQR: interquartile range, PSA: prostate-specific antigen. Study protocol URL: <https://www.prias-project.org>

Characteristic	Value
Total centers	> 100
Total patients	7813
Upgrading (primary event)	1134
Treatment	2250
Watchful waiting	334
Loss to follow-up	249
Death (unrelated to prostate cancer)	95
Death (related to prostate cancer)	2
Median age at diagnosis (years)	66 (IQR: 61–71)
Median maximum follow-up per patient (years)	1.8 (IQR: 0.9–4.0)
Total PSA measurements	67578
Median number of PSA measurements per patient	6 (IQR: 4–12)
Median PSA value (ng/mL)	5.7 (IQR: 4.1–7.7)
Total biopsies	15686
Median number of biopsies per patient	2 (IQR: 1–2)

85 profiles of a patient, and handling missing PSA measurements after a patient  
 86 experienced upgrading. In such situations, a commonly used model is the  
 87 joint model for time-to-event and longitudinal data [14, 15, 16].

88 Our joint model consisted of two sub-models. First, a linear mixed sub-  
 89 model [18] for longitudinally measured PSA (log-transformed). Second, a  
 90 relative-risk sub-model (similar to the Cox model) for obtaining the cause-  
 91 specific upgrading-risk. We included patient age in both sub-models. In the  
 92 PSA sub-model, we fitted a unique curve to the PSA measurements of each  
 93 patient (Panel A, Figure 3). Subsequently, we calculated the mathematical  
 94 derivative of the patient’s fitted PSA profile (Equation 2, Supplementary A),  
 95 to obtain his follow-up time specific instantaneous PSA velocity (Panel B,  
 96 Figure 3). This instantaneous velocity is a stronger predictor of upgrading  
 97 than the widely used average PSA velocity [19]. We modeled the impact  
 98 of PSA on upgrading-risk by employing fitted PSA value and instantaneous  
 99 velocity as predictors in the risk sub-model. Also, we included the time of  
 100 the latest negative biopsy in the risk sub-model (Panel C, Figure 3). The  
 101 parameters of the two sub-models were estimated jointly (Supplementary A)  
 102 using the R package **JMbayes** [20].

### 103 *2.3. Risk Prediction and Model Validation*

104 Our model provides predictions for upgrading-risk over the entire fu-  
 105 ture follow-up period of a patient. Predictions also automatically update  
 106 over follow-up as more patient data becomes available (Figure 5, Supple-  
 107 mentary B). We validated our PRIAS based model internally in the PRIAS  
 108 cohort, and externally in the largest six GAP3 database cohorts. We em-  
 109 ployed calibration plots [21, 22] and follow-up *time-dependent* mean absolute

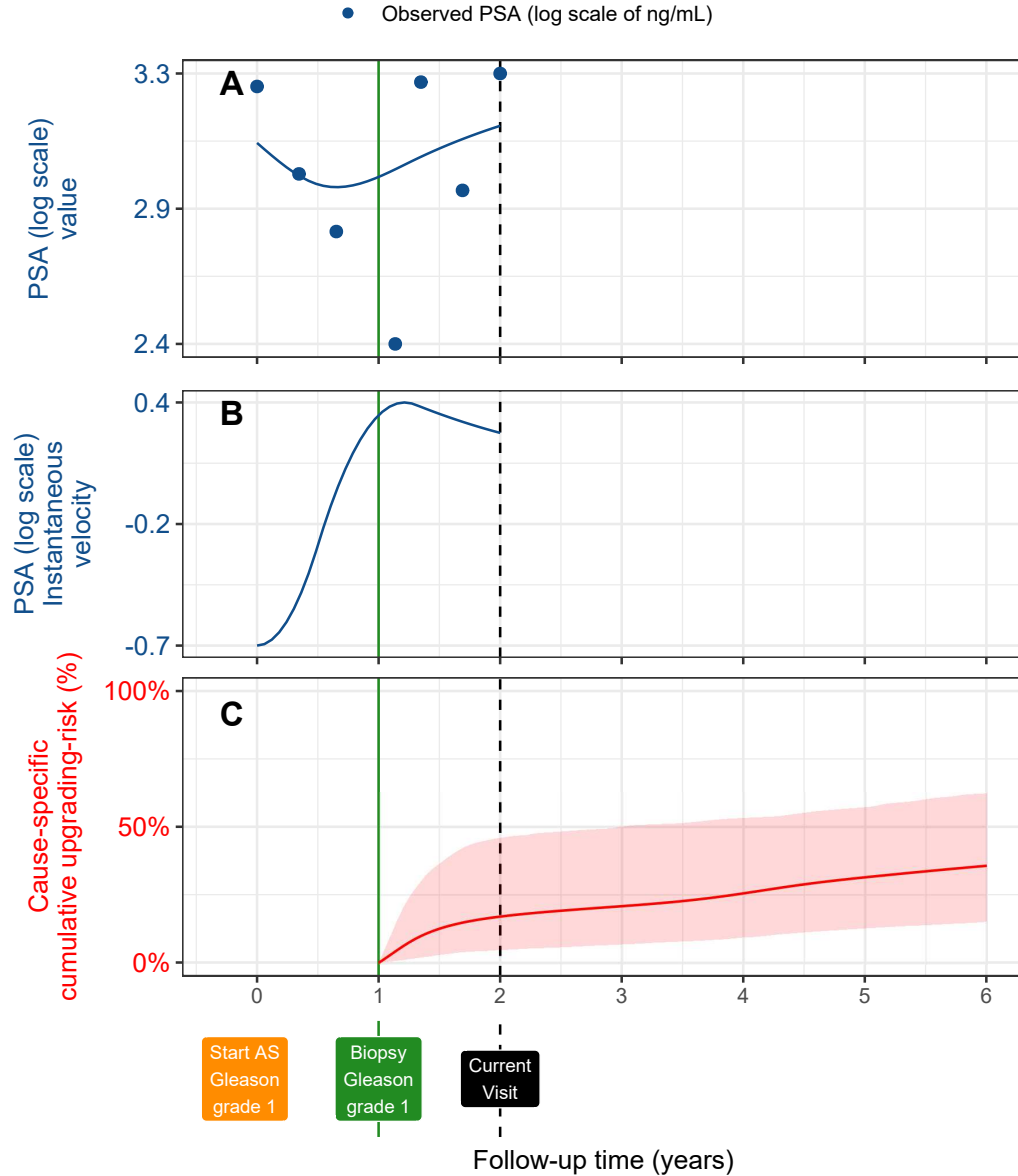


Figure 3: **Illustration of the joint model on a real PRIAS patient.** **Panel A:** Observed PSA (blue dots) and fitted PSA (solid blue line), log-transformed from ng/mL. **Panel B:** Estimated instantaneous velocity of PSA (log-transformed). **Panel C:** Predicted cause-specific cumulative upgrading-risk (95% credible interval shaded). Upgrading is defined as an increase in the Gleason grade group from group 1 [2] to 2 or higher. This upgrading-risk is calculated starting from the time of the latest negative biopsy (vertical green line at year one of follow-up). The joint model estimated it by combining the fitted PSA (log scale) value and instantaneous velocity, and time of the latest negative biopsy. Black dashed line at year two denotes the time of current visit.

110 risk prediction error or MAPE [23] to graphically and quantitatively evaluate  
 111 our model’s risk prediction accuracy, respectively. We assessed our model’s  
 112 ability to discriminate between patients who experience/do not experience  
 113 upgrading via the time-dependent area under the receiver operating charac-  
 114 teristic curve or AUC [23].

115 The aforementioned *time-dependent* AUC and MAPE [23] are temporal  
 116 extensions of their standard versions [22] in a longitudinal setting. Specif-  
 117 ically, at every six months of follow-up, we calculated a unique AUC and  
 118 MAPE for predicting upgrading-risk in the subsequent one year (Supplemen-  
 119 tary B.1). For emulating a realistic situation, we calculated the AUC and  
 120 MAPE at each follow-up using only the validation data available until that  
 121 follow-up. Last, to resolve any potential model miscalibration in validation  
 122 cohorts, we aimed to recalibrate our model’s baseline hazard of upgrading  
 123 (Supplementary B.1), individually for each cohort.

### 124 3. Results

125 The cause-specific cumulative upgrading-risk at year five of follow-up was  
 126 35% in PRIAS and at most 50% in validation cohorts (Panel B, Figure 4).  
 127 Hence, many patients do not require all biopsies planned in the first five  
 128 years of AS. In the fitted PRIAS model, the adjusted hazard ratio (aHR)  
 129 of upgrading for an increase in patient age from 61 to 71 years (25-th to  
 130 75-th percentile) was 1.45 (95%CI: 1.30–1.63). For an increase in fitted PSA  
 131 value from 2.36 to 3.07 (25-th to 75-th percentile, log scale), the aHR was  
 132 0.99 (95%CI: 0.89–1.11). The strongest predictor of upgrading-risk was in-  
 133 stantaneous PSA velocity, with an increase from -0.09 to 0.31 (25-th to 75-th

percentile), giving an aHR of 2.47 (95%CI: 1.93–2.99). The aHR for PSA value and velocity varied between GAP3 cohorts (Supplementary Table 8).

The time-dependent AUC, calibration plot, and time-dependent MAPE of our model are shown in Figure 4, and Supplementary Figure 8. In all cohorts, time-dependent AUC was moderate (0.55 to 0.75) over the whole follow-up period. Time-dependent MAPE was large (0.3 to 0.45) in those cohorts where the impact of PSA on upgrading-risk was different from PRIAS (e.g., MUSIC cohort, Supplementary Table 8), and moderate (0.1 to 0.3) otherwise. In all cohorts, the MAPE decreased rapidly after year one of follow-up. Our model was miscalibrated for validation cohorts (Panel B, Figure 4). Recalibrating the baseline hazard of upgrading in validation cohorts resolved this issue (Supplementary Figure 6). We compared risk predictions from the recalibrated models, with predictions from separately fitted cohort-specific joint models (Supplementary Figure 7). The difference in predictions was lowest in Johns Hopkins cohort (impact of PSA on upgrading-risk similar to PRIAS). Comprehensive results are in Supplementary A.2 and B.

### 3.1. *Personalized Biopsy Schedules*

We employed the PRIAS based fitted model to create personalized biopsy schedules for real PRIAS patients. Specifically, first using the model and patient’s observed data, we predicted his cumulative upgrading-risk (Figure 5) on all of his future follow-up visits (biannually in PRIAS). Subsequently, we planned biopsies on those future visits where his conditional cumulative upgrading-risk was more than a certain threshold (Supplementary Figure 9). Example personalized schedules based on 5% and 10% risk thresholds are shown in Figure 5, and in Supplementary Figure 10–12. For both personal-

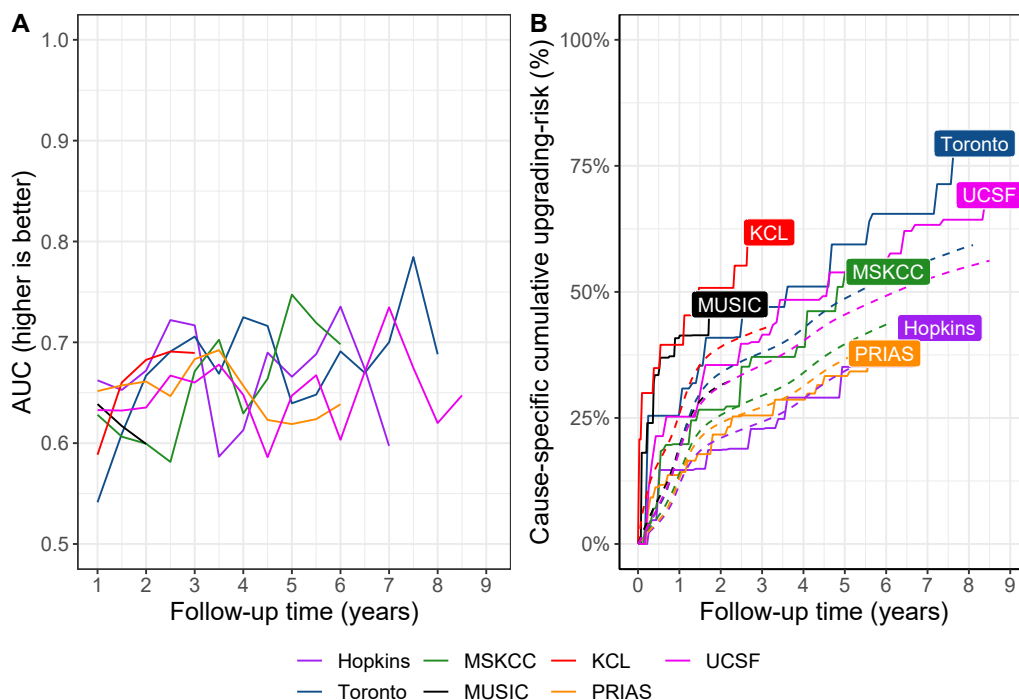


Figure 4: **Model Validation Results.** **Panel A:** time-dependent area under the receiver operating characteristic curve or AUC (measure of discrimination). **Panel B:** calibration-at-large indicates model miscalibration. This is because solid lines depicting the non-parametric estimate of the cause-specific cumulative upgrading-risk [24], and dashed lines showing the average cause-specific cumulative upgrading-risk obtained using the joint model fitted to the PRIAS dataset, are not overlapping. Recalibrating the baseline hazard of upgrading resolved this issue (Supplementary Figure 6). Full names of Cohorts are *PRIAS*: Prostate Cancer International Active Surveillance, *Toronto*: University of Toronto Active Surveillance, *Hopkins*: Johns Hopkins Active Surveillance, *MSKCC*: Memorial Sloan Kettering Cancer Center Active Surveillance, *KCL*: King’s College London Active Surveillance, *MUSIC*: Michigan Urological Surgery Improvement Collaborative Active Surveillance, *UCSF*: University of California San Francisco AS.

159 ized and fixed schedules, we estimated the expected time delay in detecting  
 160 upgrading if the patient progresses before the time of the last planned biopsy  
 161 (Panel C, Figure 5). This delay is also personalized (Supplementary C.1).  
 162 That is, even if two different patients are prescribed the same biopsy schedule,  
 163 their expected delays will depend on their individual upgrading-risk profiles.  
 164 Patients/doctors can utilize the expected delay and schedule of biopsies as  
 165 criteria to compare fixed, and different risk-based personalized schedules.

### 166 *3.2. Web-Application*

167 We implemented our model and personalized schedules in a user-friendly  
 168 web-application [https://emcbiostatistics.shinyapps.io/prias\\_biopsy\\_](https://emcbiostatistics.shinyapps.io/prias_biopsy_recommender/)  
 169 **recommender/**. Currently, the web-application supports PRIAS and the six  
 170 validation cohorts. Patient data can be entered manually and in Microsoft  
 171 Excel format. Predictions for upgrading-risk are available for a currently  
 172 limited, cohort-specific, follow-up period (Supplementary Table 9). The web-  
 173 application visualizes the timing of biopsies, and expected time delay in de-  
 174 tecting upgrading, for personalized schedules based on 5%, 10%, and 15%  
 175 risk threshold; annual biopsies; biennial biopsies; and PRIAS schedule.

## 176 **4. Discussion**

177 We successfully developed and externally validated a model for predicting  
 178 upgrading-risk [3] in prostate cancer AS, and providing risk-based personal-  
 179 ized biopsy decisions. Our work has four novel features over earlier risk  
 180 calculators [15, 25]. First, our model was fitted to the world’s largest AS  
 181 dataset PRIAS and externally validated in the largest six cohorts of the  
 182 Movember Foundation’s GAP3 database [17]. Second, the model predicts a



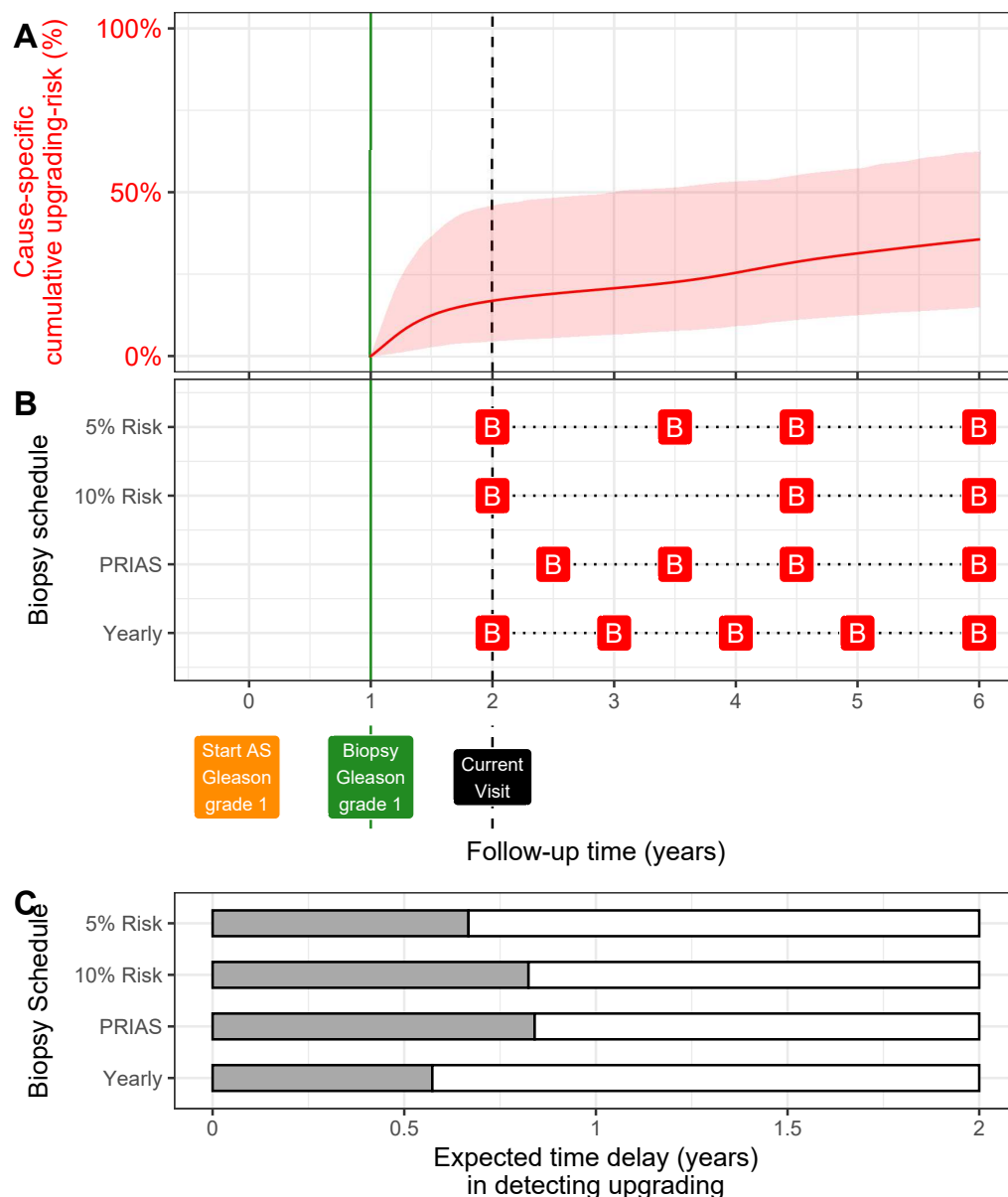


Figure 5: **Illustration of personalized and fixed schedules of biopsies for patient from Figure 3.** **Panel A:** Predicted cumulative upgrading-risk (95% credible interval shaded). **Panel B:** Different biopsy schedules with a red 'B' indicating a future biopsy. Risk: 5% and Risk: 10% are personalized schedules in which a biopsy is planned whenever the conditional cause-specific cumulative upgrading-risk is above 5% or 10% risk, respectively. Green vertical line at year one is the time of the latest negative biopsy. Black dashed line at year two denotes the time of the current visit. **Panel C:** Expected time delay in detecting upgrading (years) if patient progresses before year six. A compulsory biopsy was scheduled at year six (maximum biopsy scheduling time in PRIAS, Supplementary C) in all schedules for a meaningful comparison between them.

183 patient’s current and future upgrading-risk in a personalized manner. Third,  
 184 using the predicted risks, we created personalized biopsy schedules and also  
 185 calculated the expected time delay in detecting upgrading (less is beneficial)  
 186 if that schedule was followed. Thus, patients/doctors can compare sched-  
 187 ules before making a choice. Fourth, we implemented our methodology in a  
 188 user-friendly web-application ([https://emcbiostatistics.shinyapps.io/  
 189 prias\\_biopsy\\_recommender/](https://emcbiostatistics.shinyapps.io/prias_biopsy_recommender/)) for both PRIAS and validated cohorts.

190 Our model is useful for numerous patients from PRIAS and validated  
 191 cohorts. The discrimination ability of our model, exhibited by the *time-*  
 192 *dependent* AUC, was moderate (0.55–0.75). This is possible because, unlike  
 193 the standard AUC [22], the time-dependent AUC utilizes only the validation  
 194 data available until the time at which it is calculated. The same holds for the  
 195 time-dependent MAPE (mean absolute prediction error). Although, MAPE  
 196 varied much more between cohorts than AUC. In cohorts where the effect  
 197 size for the impact of PSA value and velocity on upgrading-risk was similar  
 198 to that for PRIAS (e.g., Hopkins cohort), MAPE was moderate. Otherwise,  
 199 MAPE was large (e.g., KCL and MUSIC cohorts). In all cohorts, MAPE  
 200 decreased rapidly after year one of follow-up. A plausible reason is that at  
 201 year one, the validation data also contains those patients who may have been  
 202 misclassified as Gleason grade group 1 at the time of inclusion in AS. This  
 203 issue can be obviated by scheduling a compulsory biopsy at year one for all  
 204 patients (current PRIAS recommendation). Last, we required recalibration  
 205 of our model’s baseline hazard of upgrading for all validation cohorts.

206 The clinical implications of our work are as follows. First, the cause-  
 207 specific cumulative upgrading-risk at year five of follow-up was at most 50%

208 in all cohorts (Panel B, Figure 4). That is, many patients may not require  
 209 all biopsies planned in the first five years of AS. Given the non-compliance  
 210 and burden of frequent biopsies [8], the availability of our methodology as a  
 211 web-application may encourage patients/doctors to consider upgrading-risk  
 212 based personalized schedules instead. An additional advantage of personal-  
 213 ized schedules is that they update as more patient data becomes available  
 214 over follow-up. We have shown via a simulation study [26] that personalized  
 215 schedules may reduce, on average, six biopsies compared to annual schedule  
 216 and two biopsies compared to PRIAS schedule in slow/non-progressing AS  
 217 patients, while maintaining almost the same time delay in detecting upgrad-  
 218 ing as PRIAS schedule. Personalized schedules with different risk thresholds  
 219 indeed have different performance. In this regard, to assist patients/doctors  
 220 in choosing between fixed schedules and personalized schedules based on  
 221 different risk thresholds, the web-application provides a patient-specific esti-  
 222 mate of the expected time delay in detecting upgrading, for both personalized  
 223 and fixed schedules. We hope that this will objectively address patient ap-  
 224 prehensions regarding adverse outcomes in AS.

225 This work has certain limitations. Predictions for upgrading-risk, and  
 226 personalized schedules are available only for a currently limited, cohort-  
 227 specific, follow-up period (Supplementary Table 9). This problem can be  
 228 mitigated by refitting the model with new follow-up data in the future. Re-  
 229 cently, some cohorts started utilizing MRI to explore the possibility of tar-  
 230 geting visible lesions by biopsy. Presently, the GAP3 database has limited  
 231 MRI follow-up data available. As more such data becomes available, the cur-  
 232 rent model can be extended to include MRI based predictors. We scheduled

233 biopsies using cause-specific cumulative upgrading-risk, which ignores com-  
 234 peting events such as treatment based on the number of positive biopsy cores.  
 235 Employing a competing-risk model may lead to improved personalized sched-  
 236 ules. Upgrading is susceptible to inter-observer variation too. Models which  
 237 account for this variation [15, 27] will be interesting to investigate further.  
 238 However, even with an enhanced risk prediction model, the methodology for  
 239 personalized scheduling and calculation of expected time delay (Supplemen-  
 240 tary C) need not change.

## 241 5. Conclusions

242 We successfully developed and externally validated a model for predict-  
 243 ing upgrading-risk, and providing risk-based personalized biopsy decisions,  
 244 in prostate cancer AS. The model made available via a user-friendly web-  
 245 application ([https://emcbiostatistics.shinyapps.io/prias\\_biopsy\\_recommender/](https://emcbiostatistics.shinyapps.io/prias_biopsy_recommender/))  
 246 enables shared decision making of biopsy schedules by comparing fixed and  
 247 personalized schedules on total biopsies and expected time delay in detecting  
 248 upgrading. Novel biomarkers and MRI data can be added as predictors in  
 249 the model to improve predictions in the future. Recalibration of baseline  
 250 upgrading-risk is advised for external cohorts.

## 251 Author Contributions

252 Anirudh Tomer had full access to all the data in the study and takes  
 253 responsibility for the integrity of the data and the accuracy of the data anal-  
 254 ysis.

255 *Study concept and design:* Tomer, Nieboer, Roobol, Bjartell, and Rizopoulos  
 256 *Acquisition of data:* Tomer, Nieboer, and Roobol  
 257 *Analysis and interpretation of data:* Tomer, Nieboer, and Rizopoulos  
 258 *Drafting of the manuscript:* Tomer, and Rizopoulos  
 259 *Critical revision of the manuscript for important intellectual content:* Tomer,  
 260 Nieboer, Roobol, Bjartell, Steyerberg, and Rizopoulos  
 261 *Statistical analyses:* Tomer, Nieboer, Steyerberg, and Rizopoulos  
 262 *Obtaining funding:* Roobol, Steyerberg, and Rizopoulos  
 263 *Administrative, technical or material support:* Nieboer  
 264 *Supervision:* Roobol, and Rizopoulos  
 265 *Other:* none

## 266 **Acknowledgments**

267 We thank Jozien Helleman from the Department of Urology, Erasmus  
 268 University Medical Center, for coordinating the project. The first and last  
 269 authors would like to acknowledge support by Nederlandse Organisatie voor  
 270 Wetenschappelijk Onderzoek (the national research council of the Nether-  
 271 lands) VIDI grant nr. 016.146.301, and Erasmus University Medical Cen-  
 272 ter funding. Part of this work was carried out on the Dutch national e-  
 273 infrastructure with the support of SURF Cooperative. The authors also  
 274 thank the Erasmus University Medical Center's Cancer Computational Biol-  
 275 ogy Center for giving access to their IT-infrastructure and software that was  
 276 used for the computations and data analysis in this study.

277 The PRIAS website is funded by the Prostate Cancer Research Foun-  
 278 dation, Rotterdam (SWOP). This work was supported by the Movember

Foundation. The funder did not play any role in the study design, collection,  
analysis or interpretation of data, or in the drafting of this paper.

## **Appendix A. Members of The Movember Foundations Global Action Plan Prostate Cancer Active Surveillance (GAP3) consortium**

*Principle Investigators:* Bruce Trock (Johns Hopkins University, The James Buchanan Brady Urological Institute, Baltimore, USA), Behfar Ehdaie (Memorial Sloan Kettering Cancer Center, New York, USA), Peter Carroll (University of California San Francisco, San Francisco, USA), Christopher Filson (Emory University School of Medicine, Winship Cancer Institute, Atlanta, USA), Jeri Kim / Christopher Logothetis (MD Anderson Cancer Centre, Houston, USA), Todd Morgan (University of Michigan and Michigan Urological Surgery Improvement Collaborative (MUSIC), Michigan, USA), Laurence Klotz (University of Toronto, Sunnybrook Health Sciences Centre, Toronto, Ontario, Canada), Tom Pickles (University of British Columbia, BC Cancer Agency, Vancouver, Canada), Eric Hyndman (University of Calgary, Southern Alberta Institute of Urology, Calgary, Canada), Caroline Moore (University College London & University College London Hospital Trust, London, UK), Vincent Gnanapragasam (University of Cambridge & Cambridge University Hospitals NHS Foundation Trust, Cambridge, UK), Mieke Van Hemelrijck (King's College London, London, UK & Guys and St Thomas NHS Foundation Trust, London, UK), Prokar Dasgupta (Guys and St Thomas NHS Foundation Trust, London, UK), Chris Bangma (Erasmus Medical Center, Rotterdam, The Netherlands/ representative of Prostate cancer Research International Active Surveillance (PRIAS)

303 consortium), Monique Roobol (Erasmus Medical Center, Rotterdam, The  
 304 Netherlands/ representative of Prostate cancer Research International Active  
 305 Surveillance (PRIAS) consortium), Arnauld Villers (Lille University Hospi-  
 306 tal Center, Lille, France), Antti Rannikko (Helsinki University and Helsinki  
 307 University Hospital, Helsinki, Finland), Riccardo Valdagni (Department of  
 308 Oncology and Hemato-oncology, Universit degli Studi di Milano, Radia-  
 309 tion Oncology 1 and Prostate Cancer Program, Fondazione IRCCS Istituto  
 310 Nazionale dei Tumori, Milan, Italy), Antoinette Perry (University College  
 311 Dublin, Dublin, Ireland), Jonas Hugosson (Sahlgrenska University Hospital,  
 312 Gteborg, Sweden), Jose Rubio-Briones (Instituto Valenciano de Oncologa,  
 313 Valencia, Spain), Anders Bjartell (Skne University Hospital, Malm, Swe-  
 314 den), Lukas Hefermehl (Kantonsspital Baden, Baden, Switzerland), Lee Lui  
 315 Shiong (Singapore General Hospital, Singapore, Singapore), Mark Fryden-  
 316 berg (Monash Health; Monash University, Melbourne, Australia), Yoshiyuki  
 317 Kakehi / Mikio Sugimoto (Kagawa University Faculty of Medicine, Kagawa,  
 318 Japan), Byung Ha Chung (Gangnam Severance Hospital, Yonsei University  
 319 Health System, Seoul, Republic of Korea)

320 *Pathologist:* Theo van der Kwast (Princess Margaret Cancer Centre,  
 321 Toronto, Canada). Technology Research Partners: Henk Obbink (Royal  
 322 Philips, Eindhoven, the Netherlands), Wim van der Linden (Royal Philips,  
 323 Eindhoven, the Netherlands), Tim Hulsen (Royal Philips, Eindhoven, the  
 324 Netherlands), Cees de Jonge (Royal Philips, Eindhoven, the Netherlands).

325 *Advisory Regional statisticians:* Mike Kattan (Cleveland Clinic, Cleve-  
 326 land, Ohio, USA), Ji Xinge (Cleveland Clinic, Cleveland, Ohio, USA), Ken-  
 327 neth Muir (University of Manchester, Manchester, UK), Artitaya Lophatananon

328 (University of Manchester, Manchester, UK), Michael Fahey (Epworth Health-  
 329 Care, Melbourne, Australia), Ewout Steyerberg (Erasmus Medical Center,  
 330 Rotterdam, The Netherlands), Daan Nieboer (Erasmus Medical Center, Rot-  
 331 terdam, The Netherlands); Liying Zhang (University of Toronto, Sunnybrook  
 332 Health Sciences Centre, Toronto, Ontario, Canada)

333 *Executive Regional statisticians:* Ewout Steyerberg (Erasmus Medical  
 334 Center, Rotterdam, The Netherlands), Daan Nieboer (Erasmus Medical Cen-  
 335 ter, Rotterdam, The Netherlands); Kerri Beckmann (King's College London,  
 336 London, UK & Guys and St Thomas NHS Foundation Trust, London, UK),  
 337 Brian Denton (University of Michigan, Michigan, USA), Andrew Hayen (Uni-  
 338 versity of Technology Sydney, Australia), Paul Boutros (Ontario Institute of  
 339 Cancer Research, Toronto, Ontario, Canada).

340 *Clinical Research Partners IT Experts:* Wei Guo (Johns Hopkins Uni-  
 341 versity, The James Buchanan Brady Urological Institute, Baltimore, USA),  
 342 Nicole Benfante (Memorial Sloan Kettering Cancer Center, New York, USA),  
 343 Janet Cowan (University of California San Francisco, San Francisco, USA),  
 344 Dattatraya Patil (Emory University School of Medicine, Winship Cancer In-  
 345 stitute, Atlanta, USA), Emily Tolosa (MD Anderson Cancer Centre, Hous-  
 346 ton, Texas, USA), Tae-Kyung Kim (University of Michigan and Michigan  
 347 Urological Surgery Improvement Collaborative, Ann Arbor, Michigan, USA),  
 348 Alexandre Mamedov (University of Toronto, Sunnybrook Health Sciences  
 349 Centre, Toronto, Ontario, Canada), Vincent LaPointe (University of British  
 350 Columbia, BC Cancer Agency, Vancouver, Canada), Trafford Crump (Uni-  
 351 versity of Calgary, Southern Alberta Institute of Urology, Calgary, Canada),  
 352 Vasilis Stavrinos (University College London & University College Lon-



353 don Hospital Trust, London, UK), Jenna Kimberly-Duffell (University of  
 354 Cambridge & Cambridge University Hospitals NHS Foundation Trust, Cam-  
 355 bridge, UK), Aida Santaolalla (King's College London, London, UK & Guys  
 356 and St Thomas NHS Foundation Trust, London, UK), Daan Nieboer (Eras-  
 357 mus Medical Center, Rotterdam, The Netherlands), Jonathan Olivier (Lille  
 358 University Hospital Center, Lille, France), Tiziana Rancati (Fondazione IR-  
 359 CCS Istituto Nazionale dei Tumori di Milano, Milan, Italy), Heln Ahlgren  
 360 (Sahlgrenska University Hospital, Gteborg, Sweden), Juanma Mascars (Insti-  
 361 tuto Valenciano de Oncologa, Valencia, Spain), Annica Lfgren (Skne Univer-  
 362 sity Hospital, Malm, Sweden), Kurt Lehmann (Kantonsspital Baden, Baden,  
 363 Switzerland), Catherine Han Lin (Monash University and Epworth Health-  
 364 Care, Melbourne, Australia), Hiromi Hiram (Kagawa University, Kagawa,  
 365 Japan), Kwang Suk Lee (Yonsei University College of Medicine, Gangnam  
 366 Severance Hospital, Seoul, Korea).

367 *Research Advisory Committee:* Guido Jenster (Erasmus MC, Rotterdam,  
 368 the Netherlands), Anssi Auvinen (University of Tampere, Tampere, Finland),  
 369 Anders Bjartell (Skne University Hospital, Malm, Sweden), Masoom Haider  
 370 (University of Toronto, Toronto, Canada), Kees van Bochove (The Hyve  
 371 B.V. Utrecht, Utrecht, the Netherlands), Ballentine Carter (Johns Hopkins  
 372 University, Baltimore, USA until 2018).

373 *Management team:* Sam Gledhill (Movember Foundation, Melbourne,  
 374 Australia), Mark Buzza / Michelle Koussou (Movember Foundation, Mel-  
 375 bourne, Australia), Chris Bangma (Erasmus Medical Center, Rotterdam,  
 376 The Netherlands), Monique Roobol (Erasmus Medical Center, Rotterdam,  
 377 The Netherlands), Sophie Bruinsma / Jozien Helleman (Erasmus Medical

Center, Rotterdam, The Netherlands).

## References

1. Briganti A, Fossati N, Catto JW, Cornford P, Montorsi F, Mottet N, Wirth M, Van Poppel H. Active surveillance for low-risk prostate cancer: the European Association of Urology position in 2018. *European urology* 2018;74(3):357–68.
2. Epstein JI, Egevad L, Amin MB, Delahunt B, Srigley JR, Humphrey PA. The 2014 international society of urological pathology (isup) consensus conference on gleason grading of prostatic carcinoma. *The American journal of surgical pathology* 2016;40(2):244–52.
3. Bruinsma SM, Roobol MJ, Carroll PR, Klotz L, Pickles T, Moore CM, Gnanapragasam VJ, Villers A, Rannikko A, Valdagni R, et al. Expert consensus document: semantics in active surveillance for men with localized prostate cancer results of a modified delphi consensus procedure. *Nature reviews urology* 2017;14(5):312.
4. Bul M, Zhu X, Valdagni R, Pickles T, Kakehi Y, Rannikko A, Bjartell A, Van Der Schoot DK, Cornel EB, Conti GN, et al. Active surveillance for low-risk prostate cancer worldwide: the prias study. *European urology* 2013;63(4):597–603.
5. Nieboer D, Tomer A, Rizopoulos D, Roobol MJ, Steyerberg EW. Active surveillance: a review of risk-based, dynamic monitoring. *Translational andrology and urology* 2018;7(1):106–15.

- 400 6. Loeb S, Carter HB, Schwartz M, Fagerlin A, Braithwaite RS, Lepor H.  
401 Heterogeneity in active surveillance protocols worldwide. *Reviews in*  
402 *urology* 2014;16(4):202–3.
- 403 7. Loeb S, Vellekoop A, Ahmed HU, Catto J, Emberton M, Nam R, Rosario  
404 DJ, Scattoni V, Lotan Y. Systematic review of complications of prostate  
405 biopsy. *European urology* 2013;64(6):876–92.
- 406 8. Bokhorst LP, Alberts AR, Rannikko A, Valdagni R, Pickles T, Kakehi Y,  
407 Bangma CH, Roobol MJ, PRIAS study group . Compliance rates with  
408 the Prostate Cancer Research International Active Surveillance (PRIAS)  
409 protocol and disease reclassification in noncompliers. *European Urology*  
410 2015;68(5):814–21.
- 411 9. Inoue LY, Lin DW, Newcomb LF, Leonardson AS, Ankerst D, Gulati R,  
412 Carter HB, Trock BJ, Carroll PR, Cooperberg MR, et al. Comparative  
413 analysis of biopsy upgrading in four prostate cancer active surveillance  
414 cohorts. *Annals of internal medicine* 2018;168(1):1–9.
- 415 10. Bratt O, Carlsson S, Holmberg E, Holmberg L, Johansson E, Josefsson  
416 A, Nilsson A, Nyberg M, Robinson D, Sandberg J, et al. The study of  
417 active monitoring in sweden (sams): a randomized study comparing two  
418 different follow-up schedules for active surveillance of low-risk prostate  
419 cancer. *Scandinavian journal of urology* 2013;47(5):347–55.
- 420 11. de Carvalho TM, Heijnsdijk EA, de Koning HJ. Estimating the risks  
421 and benefits of active surveillance protocols for prostate cancer: a mi-  
422 crosimulation study. *BJU international* 2017;119(4):560–6.

- 423 12. Partin AW, Yoo J, Carter HB, Pearson JD, Chan DW, Epstein JI, Walsh  
 424 PC. The use of prostate specific antigen, clinical stage and gleason score  
 425 to predict pathological stage in men with localized prostate cancer. *The*  
 426 *Journal of urology* 1993;150(1):110–4.
- 427 13. Makarov DV, Trock BJ, Humphreys EB, Mangold LA, Walsh PC, Ep-  
 428 stein JI, Partin AW. Updated nomogram to predict pathologic stage of  
 429 prostate cancer given prostate-specific antigen level, clinical stage, and  
 430 biopsy gleason score (partin tables) based on cases from 2000 to 2005.  
 431 *Urology* 2007;69(6):1095–101.
- 432 14. Tomer A, Nieboer D, Roobol MJ, Steyerberg EW, Rizopoulos D. Per-  
 433 sonalized schedules for surveillance of low-risk prostate cancer patients.  
 434 *Biometrics* 2019;75(1):153–62.
- 435 15. Coley RY, Zeger SL, Mamawala M, Pienta KJ, Carter HB. Prediction  
 436 of the pathologic gleason score to inform a personalized management  
 437 program for prostate cancer. *European urology* 2017;72(1):135–41.
- 438 16. Rizopoulos D. Joint Models for Longitudinal and Time-to-Event Data:  
 439 With Applications in R. CRC Press; 2012. ISBN 9781439872864.
- 440 17. Bruinsma SM, Zhang L, Roobol MJ, Bangma CH, Steyerberg EW,  
 441 Nieboer D, Van Hemelrijck M, consortium MFGAPPCASG, Trock B,  
 442 Ehdaie B, et al. The movember foundation’s gap3 cohort: a profile of  
 443 the largest global prostate cancer active surveillance database to date.  
 444 *BJU international* 2018;121(5):737–44.

- 445 18. Laird NM, Ware JH, et al. Random-effects models for longitudinal data.  
446 *Biometrics* 1982;38(4):963–74.
- 447 19. Cooperberg MR, Brooks JD, Faino AV, Newcomb LF, Kearns JT, Car-  
448 roll PR, Dash A, Etzioni R, Fabrizio MD, Gleave ME, et al. Refined  
449 analysis of prostate-specific antigen kinetics to predict prostate cancer  
450 active surveillance outcomes. *European urology* 2018;74(2):211–7.
- 451 20. Rizopoulos D. The R package JMBayes for fitting joint models for lon-  
452 gitudinal and time-to-event data using MCMC. *Journal of Statistical*  
453 *Software* 2016;72(7):1–46.
- 454 21. Royston P, Altman DG. External validation of a cox prognostic  
455 model: principles and methods. *BMC medical research methodology*  
456 2013;13(1):33.
- 457 22. Steyerberg EW, Vickers AJ, Cook NR, Gerds T, Gonen M, Obuchowski  
458 N, Pencina MJ, Kattan MW. Assessing the performance of prediction  
459 models: a framework for some traditional and novel measures. *Epidemi-*  
460 *ology (Cambridge, Mass)* 2010;21(1):128.
- 461 23. Rizopoulos D, Molenberghs G, Lesaffre EM. Dynamic predictions with  
462 time-dependent covariates in survival analysis using joint modeling and  
463 landmarking. *Biometrical Journal* 2017;59(6):1261–76.
- 464 24. Turnbull BW. The empirical distribution function with arbitrarily  
465 grouped, censored and truncated data. *Journal of the Royal Statisti-*  
466 *cal Society Series B (Methodological)* 1976;38(3):290–5.

- 467 25. Ankerst DP, Xia J, Thompson Jr IM, Hoeffler J, Newcomb LF, Brooks  
468 JD, Carroll PR, Ellis WJ, Gleave ME, Lance RS, et al. Precision  
469 medicine in active surveillance for prostate cancer: development of the  
470 canary–early detection research network active surveillance biopsy risk  
471 calculator. *European urology* 2015;68(6):1083–8.
- 472 26. Tomer A, Rizopoulos D, Nieboer D, Drost FJ, Roobol MJ, Steyerberg  
473 EW. Personalized decision making for biopsies in prostate cancer active  
474 surveillance programs. *Medical Decision Making* 2019;39(5):499–508.
- 475 27. Balasubramanian R, Lagakos SW. Estimation of a failure time distribu-  
476 tion based on imperfect diagnostic tests. *Biometrika* 2003;90(1):171–82.

Supplementary File containing full results, and extra figures referred in the main manuscript begins here onwards.

# Supplementary Materials for “A Ready To Use Web-Application Providing a Personalized Biopsy Schedule for Men With Low-Risk PCa Under Active Surveillance”

Anirudh Tomer, MSc<sup>a,\*</sup>, Daan Nieboer, MSc<sup>b</sup>, Monique J. Roobol, PhD<sup>c</sup>,  
Anders Bjartell, MD, PhD<sup>d</sup>, Ewout W. Steyerberg, PhD<sup>b,e</sup>, Dimitris  
Rizopoulos, PhD<sup>a</sup>, Movember Foundation’s Global Action Plan Prostate  
Cancer Active Surveillance (GAP3) consortium<sup>f</sup>

<sup>a</sup>*Department of Biostatistics, Erasmus University Medical Center, Rotterdam, the  
Netherlands*

<sup>b</sup>*Department of Public Health, Erasmus University Medical Center, Rotterdam, the  
Netherlands*

<sup>c</sup>*Department of Urology, Erasmus University Medical Center, Rotterdam, the Netherlands*

<sup>d</sup>*Department of Urology, Skåne University Hospital, Malmö, Sweden*

<sup>e</sup>*Department of Biomedical Data Sciences, Leiden University Medical Center, Leiden, the  
Netherlands*

<sup>f</sup>*The Movember Foundation’s Global Action Plan Prostate Cancer Active Surveillance  
(GAP3) consortium members presented in Appendix F*

---

## 1 **Appendix A. A Joint Model for the Longitudinal PSA, and Time** 2 **to Gleason Upgrading**

3 Let  $T_i^*$  denote the true time of upgrading (increase in biopsy Gleason  
4 grade group from 1 to 2 or higher) for the  $i$ -th patient included in PRIAS.  
5 Since biopsies are conducted periodically,  $T_i^*$  is observed with interval cen-  
6 soring  $l_i < T_i^* \leq r_i$ . When upgrading is observed for the patient at his latest

---

\*Corresponding author (Anirudh Tomer): Erasmus MC, kamer flex Na-2823, PO Box  
2040, 3000 CA Rotterdam, the Netherlands. Tel: +31 10 70 43393

*Email addresses:* [a.tomer@erasmusmc.nl](mailto:a.tomer@erasmusmc.nl) (Anirudh Tomer, MSc),  
[d.nieboer@erasmusmc.nl](mailto:d.nieboer@erasmusmc.nl) (Daan Nieboer, MSc), [m.roobol@erasmusmc.nl](mailto:m.roobol@erasmusmc.nl) (Monique J.  
Roobol, PhD), [anders.bjartell@med.lu.se](mailto:anders.bjartell@med.lu.se) (Anders Bjartell, MD, PhD),  
[e.w.steyerberg@lumc.nl](mailto:e.w.steyerberg@lumc.nl) (Ewout W. Steyerberg, PhD), [d.rizopoulos@erasmusmc.nl](mailto:d.rizopoulos@erasmusmc.nl)  
(Dimitris Rizopoulos, PhD)



7 biopsy time  $r_i$ , then  $l_i$  denotes the time of the second latest biopsy. Oth-  
 8 erwise,  $l_i$  denotes the time of the latest biopsy and  $r_i = \infty$ . Let  $\mathbf{y}_i$  denote  
 9 his observed PSA longitudinal measurements. The observed data of all  $n$   
 10 patients is denoted by  $\mathcal{A}_n = \{l_i, r_i, \mathbf{y}_i; i = 1, \dots, n\}$ .

In our joint model, the patient-specific PSA measurements over time are modeled using a linear mixed effects sub-model. It is given by (see Panel A, Figure 1):

$$\begin{aligned} \log_2 \{y_i(t) + 1\} &= m_i(t) + \varepsilon_i(t), \\ m_i(t) &= \beta_0 + b_{0i} + \sum_{k=1}^4 (\beta_k + b_{ki}) B_k\left(\frac{t-2}{2}, \frac{\mathcal{K}-2}{2}\right) + \beta_5 \text{age}_i, \end{aligned} \quad (1)$$

11 where,  $m_i(t)$  denotes the measurement error free value of  $\log_2(\text{PSA}+1)$  trans-  
 12 formed [2, 3] measurements at time  $t$ . We model it non-linearly over time us-  
 13 ing B-splines [4]. To this end, our B-spline basis function  $B_k\{(t-2)/2, (\mathcal{K}-2)/2\}$   
 14 has three internal knots at  $\mathcal{K} = \{0.5, 1.3, 3\}$  years, which are the three quar-  
 15 tiles of the observed follow-up times. The boundary knots of the spline are  
 16 at 0 and 6.3 years (95-th percentile of the observed follow-up times). We  
 17 mean centered (mean 2 years) and standardized (standard deviation 2 years)  
 18 the follow-up time  $t$  and the knots of the B-spline  $\mathcal{K}$  during parameter esti-  
 19 mation for better convergence. The fixed effect parameters are denoted by  
 20  $\{\beta_0, \dots, \beta_5\}$ , and  $\{b_{0i}, \dots, b_{4i}\}$  are the patient specific random effects. The  
 21 random effects follow a multivariate normal distribution with mean zero and  
 22 variance-covariance matrix  $\mathbf{W}$ . The error  $\varepsilon_i(t)$  is assumed to be t-distributed  
 23 with three degrees of freedom (see Appendix B.1) and scale  $\sigma$ , and is inde-  
 24 pendent of the random effects.

To model the impact of PSA measurements on the risk of upgrading, our joint model uses a relative risk sub-model. More specifically, the hazard of upgrading denoted as  $h_i(t)$ , and the cumulative-risk of upgrading denoted as  $R_i(t)$ , at a time  $t$  are (see Panel C, Figure 1):

$$\begin{aligned} h_i(t) &= h_0(t) \exp \left( \gamma \text{age}_i + \alpha_1 m_i(t) + \alpha_2 \frac{dm_i(t)}{dt} \right), \\ R_i(t) &= \exp \left\{ - \int_0^t h_i(s) ds \right\}, \end{aligned} \quad (2)$$

where,  $\gamma$  is the parameter for the effect of age. The impact of PSA on the hazard of upgrading is modeled in two ways, namely the impact of the error

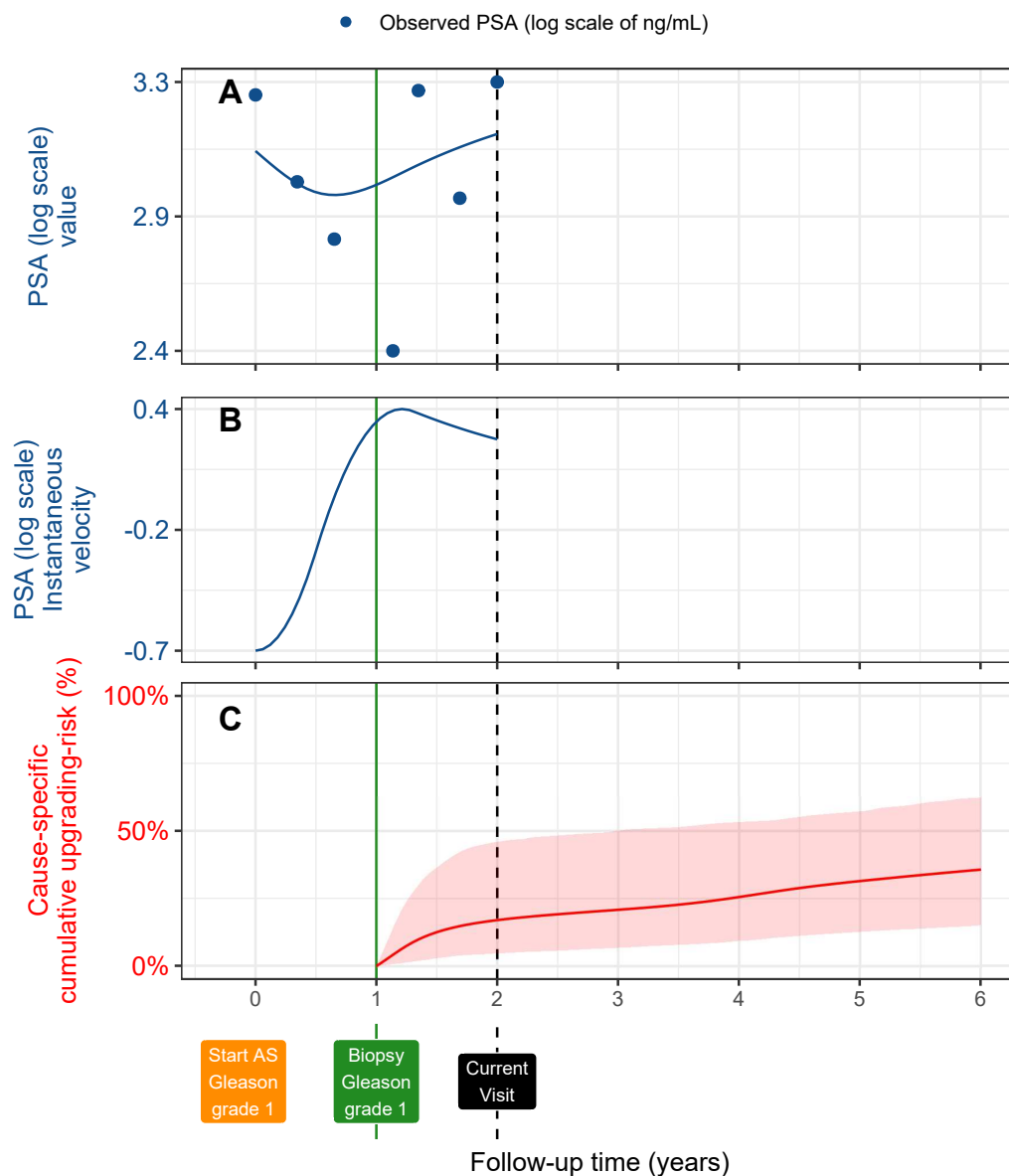


Figure 1: **Illustration of the joint model on a real PRIAS dataset patient.** **Panel A:** Observed (blue dots) and fitted PSA (solid blue line) measurements, log-transformed. **Panel B:** Estimated instantaneous velocity of PSA (log-transformed). **Panel C:** Predicted cumulative-risk of upgrading (95% credible interval shaded). Upgrading is defined as an increase in Gleason grade group [1] from grade group 1 to 2 or higher. This risk of upgrading is available starting from the time of the latest negative biopsy (vertical green line at year 1 of follow-up). The joint model estimated it by combining the fitted PSA value and velocity (both on the log scale of PSA) and time of the latest negative biopsy. Black dashed line at year 4 denotes the time of current visit.

free underlying PSA value  $m_i(t)$  (see Panel A, Figure 1), and the impact of the underlying PSA velocity  $dm_i(t)/dt$  (see Panel B, Figure 1). The corresponding parameters are  $\alpha_1$  and  $\alpha_2$ , respectively. Lastly,  $h_0(t)$  is the baseline hazard at time  $t$ , and is modeled flexibly using P-splines [5]. More specifically:

$$\log h_0(t) = \gamma_{h_0,0} + \sum_{q=1}^Q \gamma_{h_0,q} B_q(t, \mathbf{v}),$$

25 where  $B_q(t, \mathbf{v})$  denotes the  $q$ -th basis function of a B-spline with knots  $\mathbf{v} =$   
 26  $v_1, \dots, v_Q$  and vector of spline coefficients  $\gamma_{h_0}$ . To avoid choosing the number  
 27 and position of knots in the spline, a relatively high number of knots (e.g.,  
 28 15 to 20) are chosen and the corresponding B-spline regression coefficients  
 29  $\gamma_{h_0}$  are penalized using a differences penalty [5].

We estimate the parameters of the joint model using Markov chain Monte Carlo (MCMC) methods under the Bayesian framework. Let  $\boldsymbol{\theta}$  denote the vector of all of the parameters of the joint model. The joint model postulates that given the random effects, the time of upgrading, and the PSA measurements taken over time are all mutually independent. Under this assumption the posterior distribution of the parameters is given by:

$$\begin{aligned} p(\boldsymbol{\theta}, \mathbf{b} \mid \mathcal{A}_n) &\propto \prod_{i=1}^n p(l_i, r_i, \mathbf{y}_i \mid \mathbf{b}_i, \boldsymbol{\theta}) p(\mathbf{b}_i \mid \boldsymbol{\theta}) p(\boldsymbol{\theta}) \\ &\propto \prod_{i=1}^n p(l_i, r_i \mid \mathbf{b}_i, \boldsymbol{\theta}) p(\mathbf{y}_i \mid \mathbf{b}_i, \boldsymbol{\theta}) p(\mathbf{b}_i \mid \boldsymbol{\theta}) p(\boldsymbol{\theta}), \\ p(\mathbf{b}_i \mid \boldsymbol{\theta}) &= \frac{1}{\sqrt{(2\pi)^q \det(\mathbf{W})}} \exp \left\{ -\frac{1}{2} (\mathbf{b}_i^T \mathbf{W}^{-1} \mathbf{b}_i) \right\}, \end{aligned}$$

where, the likelihood contribution of the PSA outcome, conditional on the random effects is:

$$p(\mathbf{y}_i \mid \mathbf{b}_i, \boldsymbol{\theta}) = \frac{1}{(\sqrt{2\pi}\sigma^2)^{n_i}} \exp \left\{ -\frac{\sum_{j=1}^{n_i} (y_{ij} - m_{ij})^2}{2\sigma^2} \right\},$$

where  $n_i$  is the number of PSA measurements of the  $i$ -th patient. The likelihood contribution of the time of upgrading outcome is given by:

$$p(l_i, r_i \mid \mathbf{b}_i, \boldsymbol{\theta}) = \exp \left\{ -\int_0^{l_i} h_i(s) ds \right\} - \exp \left\{ -\int_0^{r_i} h_i(s) ds \right\}. \quad (3)$$

30 The integrals in (3) do not have a closed-form solution, and therefore we use  
 31 a 15-point Gauss-Kronrod quadrature rule to approximate them.

32 We use independent normal priors with zero mean and variance 100 for  
 33 the fixed effects  $\{\beta_0, \dots, \beta_5\}$ , and inverse Gamma prior with shape and rate  
 34 both equal to 0.01 for the parameter  $\sigma^2$ . For the variance-covariance matrix  
 35  $\mathbf{W}$  of the random effects, we take inverse Wishart prior with an identity scale  
 36 matrix and degrees of freedom equal to 5 (number of random effects). For  
 37 the relative risk model's parameter  $\gamma$  and the association parameters  $\alpha_1, \alpha_2$ ,  
 38 we use independent normal priors with zero mean and variance 100.

#### 39 *Appendix A.1. Assumption of t-distributed (df=3) Error Terms*

40 With regards to the choice of the distribution for the error term  $\varepsilon$  for  
 41 the PSA measurements (see Equation 1), we attempted fitting multiple joint  
 42 models differing in error distribution, namely t-distribution with three, and  
 43 four degrees of freedom, and a normal distribution for the error term. How-  
 44 ever, the model assumption for the error term was best met by the model with  
 45 t-distribution having three degrees of freedom. The quantile-quantile plot of  
 46 subject-specific residuals for the corresponding model in Panel A of Figure 2,  
 47 shows that the assumption of t-distributed (df=3) errors is reasonably met  
 48 by the fitted model.

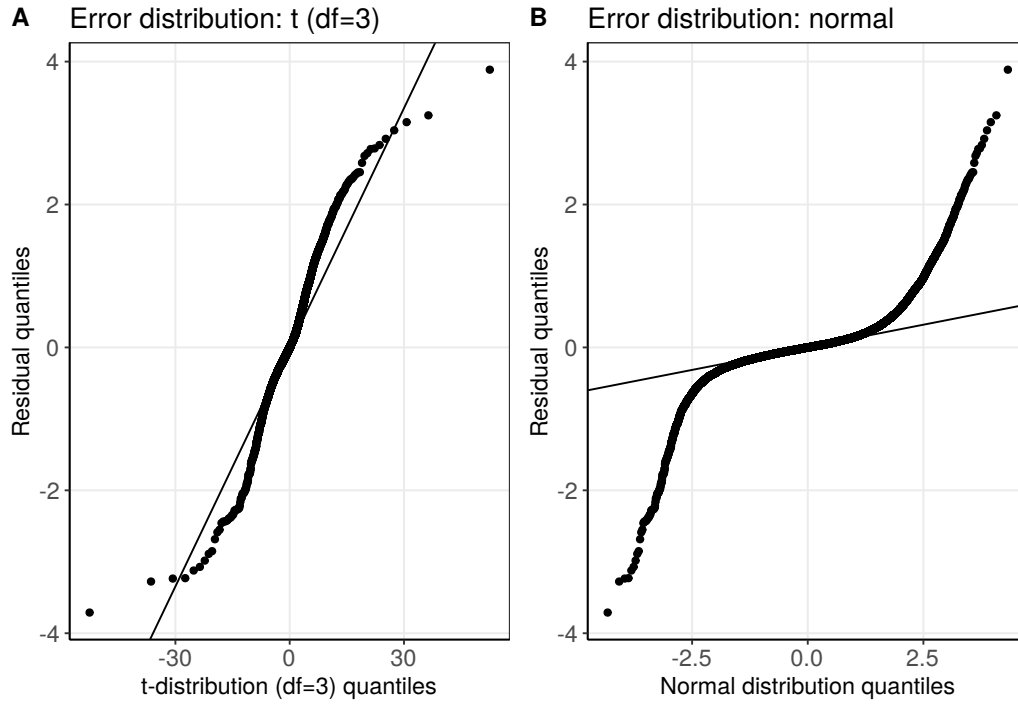


Figure 2: **Quantile-quantile plot** of subject-specific PSA residuals from two different joint models fitted to the PRIAS dataset. **Panel A:** model assuming a t-distribution (df=3) for the error term  $\varepsilon$  (see Equation 1). **Panel B:** model assuming a normal distribution for the error term  $\varepsilon$ . We selected the model with t-distributed error terms.

49 *Appendix A.2. Results*

50 Characteristics of the six validation cohorts from the GAP3 database [6]  
 51 are shown in Table 1, Table 2, and Table 3. The cause-specific cumulative  
 52 upgrading-risk in these cohorts is shown in Figure 3.

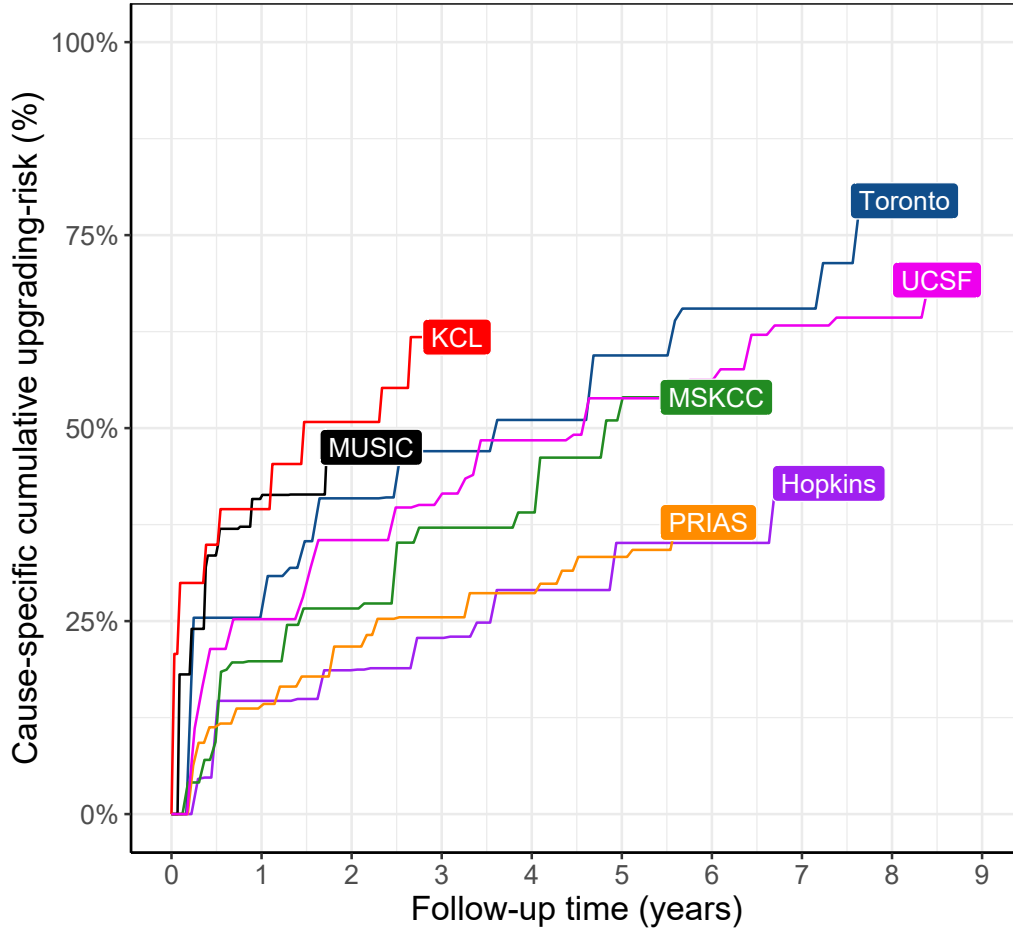


Figure 3: **Nonparametric estimate [7] of the cause-specific cumulative upgrading-risk** in the world's largest AS cohort PRIAS, and largest six AS cohorts from the GAP3 database [6]. Abbreviations are *Hopkins*: Johns Hopkins Active Surveillance, *PRIAS*: Prostate Cancer International Active Surveillance, *Toronto*: University of Toronto Active Surveillance, *MSKCC*: Memorial Sloan Kettering Cancer Center Active Surveillance, *KCL*: King's College London Active Surveillance, *MUSIC*: Michigan Urological Surgery Improvement Collaborative AS, *UCSF*: University of California San Francisco Active Surveillance.

Table 1: **Summary of the Hopkins and Toronto validation cohorts from the GAP3 database [6]**. The primary event of interest is upgrading, that is, increase in Gleason grade group from group 1 to 2 or higher. #PSA: number of PSA, #biopsies: number of biopsies, IQR: interquartile range, PSA: prostate-specific antigen. Full names of cohorts are *Hopkins*: Johns Hopkins Active Surveillance, *Toronto*: University of Toronto Active Surveillance

Characteristic	Hopkins	Toronto
Total patients	1392	1046
Upgrading (primary event)	260	359
Median age (years)	62 (IQR: 66–69)	67 (IQR: 60–72)
Median maximum follow-up per patient (years)	3 (IQR: 1.3–5.8)	4.5 (IQR: 1.9–8.4)
Total PSA measurements	11126	13984
Median #PSA per patient	6 (IQR: 4–11)	12 (IQR: 7–19)
Median PSA (ng/mL)	4.7 (IQR: 2.9–6.7)	6 (IQR: 3.7–9.0)
Total biopsies	1926	909
Median #biopsies per patient	1 (IQR: 1–2)	1 (IQR: 1–2)

Table 2: **Summary of the MSKCC and UCSF validation cohorts from the GAP3 database [6]**. The primary event of interest is upgrading, that is, increase in Gleason grade group from group 1 to 2 or higher. #PSA: number of PSA, #biopsies: number of biopsies, IQR: interquartile range, PSA: prostate-specific antigen. Full names of cohorts are *MSKCC*: Memorial Sloan Kettering Cancer Center Active Surveillance, *UCSF*: University of California San Francisco Active Surveillance.

Characteristic	MSKCC	UCSF
Total patients	894	1397
Upgrading (primary event)	242	547
Median age (years)	63 (IQR: 57–68)	63 (IQR: 57–68)
Median maximum follow-up per patient (years)	5.3 (IQR: 1.8–8.3)	3.6 (IQR: 1.5–7.2)
Total PSA measurements	10704	16093
Median #PSA per patient	11 (IQR: 5–17)	8 (IQR: 4–16)
Median PSA (ng/mL)	4.7 (IQR: 2.8–7.1)	5.0 (IQR: 3.4–7.2)
Total biopsies	1102	3512
Median #biopsies per patient	1 (IQR: 1–2)	2 (IQR: 2–3)

Table 3: **Summary of the MUSIC and KCL validation cohorts from the GAP3 database [6].** The primary event of interest is upgrading, that is, increase in Gleason grade group from group 1 to 2 or higher. #PSA: number of PSA, #biopsies: number of biopsies, IQR: interquartile range, PSA: prostate-specific antigen. Full names of cohorts are *KCL*: King’s College London Active Surveillance, *MUSIC*: Michigan Urological Surgery Improvement Collaborative AS.

Characteristic	MUSIC	KCL
Total patients	2743	616
Upgrading (primary event)	385	198
Median age (years)	65 (IQR: 60–71)	63 (IQR: 58–68)
Median maximum follow-up per patient (years)	1.2 (IQR: 0.6–2.2)	2.4 (IQR: 1.3–3.8)
Total PSA measurements	12087	2987
Median #PSA per patient	4 (IQR: 2–6)	4 (IQR: 2–6)
Median PSA (ng/mL)	5.1 (IQR: 3.4–7.1)	6 (IQR: 4–9)
Total biopsies	1032	484
Median #biopsies per patient	1 (IQR: 1–1)	1 (IQR: 1–1)

Table 4: **Estimated variance-covariance matrix  $\mathbf{W}$**  of the random effects  $\mathbf{b} = (b_0, b_1, b_2, b_3, b_4)$  from the joint model fitted to the PRIAS dataset. The variances of the random effects are highlighted along the diagonal of the variance-covariance matrix.

Random Effects	$b_0$	$b_1$	$b_2$	$b_3$	$b_4$
$b_0$	<b>0.229</b>	0.030	0.023	0.073	0.007
$b_1$	0.030	<b>0.149</b>	0.098	0.171	0.085
$b_2$	0.023	0.098	<b>0.276</b>	0.335	0.236
$b_3$	0.073	0.171	0.335	<b>0.560</b>	0.359
$b_4$	0.007	0.085	0.236	0.359	<b>0.351</b>

The joint model was fitted using the R package **JMbayes** [8]. This package utilizes the Bayesian methodology to estimate model parameters. The corresponding posterior parameter estimates are shown in Table 5 (longitudinal sub-model for PSA outcome) and Table 6 (relative risk sub-model). The parameter estimates for the variance-covariance matrix  $\mathbf{W}$  from the longitudinal sub-model for PSA are shown in the following Table 4:

For the PSA mixed effects sub-model parameter estimates (see Equation 1), in Table 5 we can see that the age of the patient trivially affects the baseline  $\log_2(\text{PSA} + 1)$  measurement. Since the longitudinal evolution of  $\log_2(\text{PSA} + 1)$  measurements is modeled with non-linear terms, the interpretation of the coefficients corresponding to time is not straightforward. In lieu of the interpretation, in Figure 4 we present plots of observed versus fitted



Table 5: **Parameters of the longitudinal sub-model:** Estimated mean and 95% credible interval for parameters in Equation (1).

Variable	Mean	Std. Dev	2.5%	97.5%	P
Intercept	2.129	0.060	2.009	2.244	<0.001
Age	0.008	0.001	0.007	0.010	<0.001
Spline: [0.0, 0.5] years	0.063	0.007	0.051	0.075	<0.001
Spline: [0.5, 1.3] years	0.196	0.010	0.177	0.217	<0.001
Spline: [1.3, 3.0] years	0.244	0.014	0.217	0.272	<0.001
Spline: [3.0, 6.3] years	0.382	0.014	0.356	0.410	<0.001
$\sigma$	0.139	0.001	0.138	0.140	

Table 6: **Parameters of the relative risk sub-model:** Estimated mean and 95% credible interval for the parameters in Equation (2).

Variable	Mean	Std. Dev	2.5%	97.5%	P
Age	0.037	0.006	0.025	0.049	<0.001
Fitted $\log_2(\text{PSA} + 1)$ value	-0.012	0.076	-0.164	0.135	0.856
Fitted $\log_2(\text{PSA} + 1)$ velocity	2.266	0.299	1.613	2.767	<0.001

65 PSA profiles for nine randomly selected patients.

66 For the relative risk sub-model (see Equation 2), the parameter estimates  
 67 in Table 6 show that  $\log_2(\text{PSA} + 1)$  velocity and age of the patient were  
 68 significantly associated with the hazard of upgrading.

69 It is important to note that since age, and  $\log_2(\text{PSA} + 1)$  value and ve-  
 70 locity are all measured on different scales, a comparison between the cor-  
 71 responding parameter estimates is not easy. To this end, in Table 7, we  
 72 present the hazard ratio of upgrading, for an increase in the aforementioned  
 73 variables from their 25-th to the 75-th percentile. For example, an increase  
 74 in fitted  $\log_2(\text{PSA} + 1)$  velocity from -0.085 to 0.308 (fitted 25-th and 75-th  
 75 percentiles) corresponds to a hazard ratio of 2.433. The interpretation of the  
 76 rest is similar.

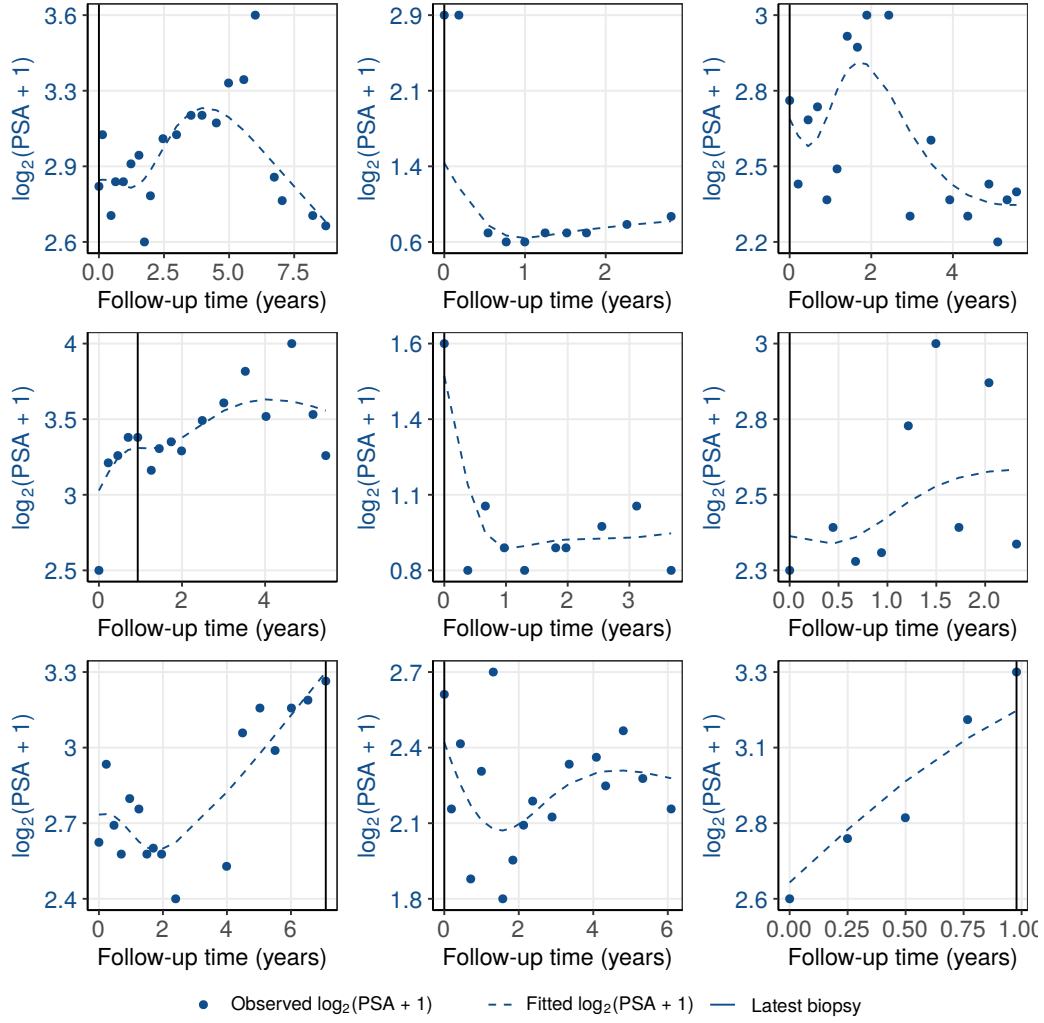


Figure 4: **Fitted versus observed  $\log_2(\text{PSA} + 1)$  profiles** for nine randomly selected PRIAS patients. The fitted profiles utilize information from the observed PSA measurements, and time of the latest biopsy.

Table 7: **Hazard ratio and 95% credible interval (CI) for upgrading:** Variables are on different scale and hence we compare an increase in the variables of relative risk sub-model from their 25-th percentile ( $P_{25}$ ) to their 75-th percentile ( $P_{75}$ ). Except for age, quartiles for all other variables are based on their fitted values obtained from the joint model fitted to the PRIAS dataset.

Variable	$P_{25}$	$P_{75}$	Hazard ratio [95% CI]
Age	61	71	1.455 [1.285, 1.631]
Fitted $\log_2(\text{PSA} + 1)$ value	2.360	3.078	0.991 [0.889, 1.102]
Fitted $\log_2(\text{PSA} + 1)$ velocity	-0.085	0.308	2.433 [1.883, 2.962]

Table 8: **Parameters of the relative risk sub-model in validation cohorts.** We fitted separate joint models for each of the six GAP3 validation cohorts as well. The specification of these joint models was same as that of the model for PRIAS. Two important predictors in the relative-risk sub-model, namely, the  $\log_2(\text{PSA} + 1)$  value and velocity have different impact on upgrading-risk across the cohorts. Table shows the mean estimate of these parameters with 95% credible interval in brackets. Strongest average effect of  $\log_2(\text{PSA} + 1)$  velocity is in PRIAS cohort, whereas the weakest is in MUSIC cohort. The strongest average effect of  $\log_2(\text{PSA} + 1)$  value is in the Toronto cohort whereas the weakest is in PRIAS cohort. Full names of cohorts are *Hopkins*: Johns Hopkins Active Surveillance, *PRIAS*: Prostate Cancer International Active Surveillance, *Toronto*: University of Toronto Active Surveillance, *MSKCC*: Memorial Sloan Kettering Cancer Center Active Surveillance, *KCL*: King's College London Active Surveillance, *MUSIC*: Michigan Urological Surgery Improvement Collaborative AS, *UCSF*: University of California San Francisco Active Surveillance.

Cohort	Fitted $\log_2(\text{PSA} + 1)$ value	Fitted $\log_2(\text{PSA} + 1)$ velocity
PRIAS	-0.012 [-0.164, 0.135]	2.266 [1.613, 2.767]
Hopkins	0.061 [-0.323, 0.329]	1.839 [0.761, 4.378]
MSKCC	0.336 [0.081, 0.583]	1.122 [0.421, 1.980]
Toronto	0.572 [0.347, 0.794]	0.943 [0.464, 1.554]
UCSF	0.498 [0.326, 0.673]	0.812 [0.280, 1.383]
MUSIC	0.441 [0.092, 0.767]	0.029 [-0.552, 0.512]
KCL	0.194 [-0.104, 0.540]	0.840 [-0.087, 1.665]

## 77 Appendix B. Risk Predictions for Upgrading

Let us assume a new patient  $j$ , for whom we need to estimate the upgrading-risk. Let his current follow-up visit time be  $v$ , latest time of biopsy be  $t$ , observed vector PSA measurements be  $\mathcal{Y}_j(v)$ . The combined information from the observed data about the time of upgrading, is given by the following posterior predictive distribution  $g(T_j^*)$  of his time  $T_j^*$  of upgrading:

$$\begin{aligned} g(T_j^*) &= p\{T_j^* \mid T_j^* > t, \mathcal{Y}_j(v), \mathcal{A}_n\} \\ &= \int \int p(T_j^* \mid T_j^* > t, \mathbf{b}_j, \boldsymbol{\theta}) p\{\mathbf{b}_j \mid T_j^* > t, \mathcal{Y}_j(v), \boldsymbol{\theta}\} p(\boldsymbol{\theta} \mid \mathcal{A}_n) d\mathbf{b}_j d\boldsymbol{\theta}. \end{aligned}$$

78 The distribution  $g(T_j^*)$  depends not only depends on the observed data of the  
 79 patient  $T_j^* > t, \mathcal{Y}_j(v)$ , but also depends on the information from the PRIAS  
 80 dataset  $\mathcal{A}_n$ . To this the the posterior distribution of random effects  $\mathbf{b}_j$  and  
 81 posterior distribution of the vector of all parameters  $\boldsymbol{\theta}$  are utilized, respec-  
 82 tively. The distribution  $g(T_j^*)$  can be estimated as detailed in Rizopoulos  
 83 et al. [9]. Since, many prostate cancer patients may not obtain upgrading  
 84 in the current follow-up period of PRIAS,  $g(T_j^*)$  can only be estimated for a  
 85 currently limited follow-up period.

The cause-specific cumulative upgrading-risk can be derived from  $g(T_j^*)$  as given in [9]. It is given by:

$$R_j(u \mid t, v) = \Pr\{T_j^* > u \mid T_j^* > t, \mathcal{Y}_j(v), \mathcal{A}_n\}, \quad u \geq t. \quad (4)$$

86 The personalized risk profile of the patient (see Panel C, Figure 5) updates  
 87 as more data is gathered over follow-up visits.

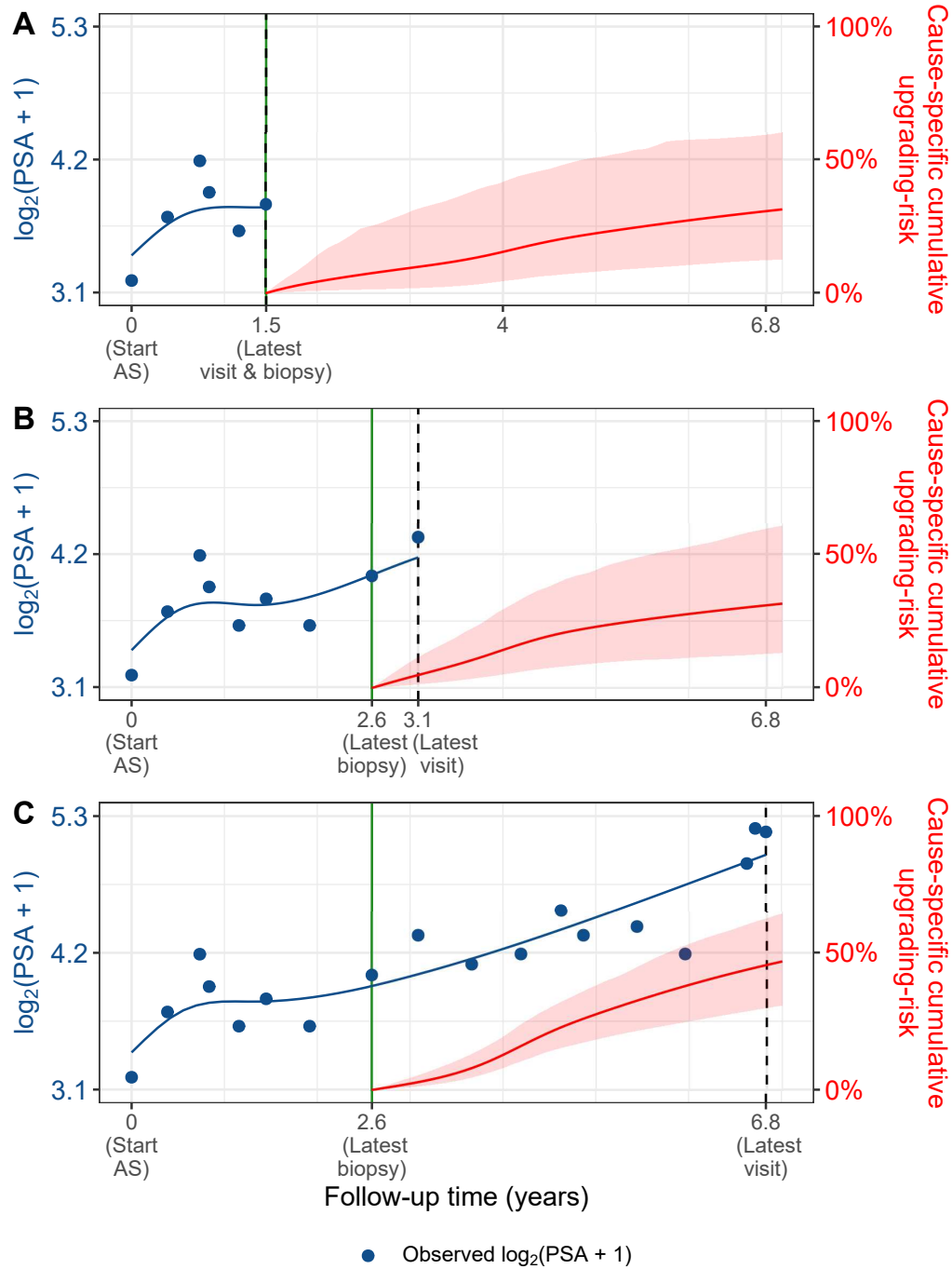


Figure 5: **Cause-specific cumulative upgrading-risk changing dynamically over follow-up** as more patient data is gathered. The three **Panels A,B and C**: are ordered by the time of the latest visit (dashed vertical black line) of a new patient. At each of the latest follow-up visits, we combine the accumulated PSA measurements (shown in blue), and latest time of negative biopsy (solid vertical green line) to obtain the updated cumulative-risk profile (shown in red) of the patient.

### 88 *Appendix B.1. Validation of Risk Predictions*

89 We wanted to check the usefulness of our model for not only the PRIAS  
 90 patients but also for patients from other cohorts. To this end, we validated  
 91 our model in the PRIAS dataset (internal validation) and the largest six co-  
 92 horts from the GAP3 database [6]. These are the University of Toronto AS  
 93 (Toronto), Johns Hopkins AS (Hopkins), Memorial Sloan Kettering Can-  
 94 cer Center AS (MSKCC), University of California San Francisco Active  
 95 Surveillance (UCSF), King’s College London AS (KCL), Michigan Urological  
 96 Surgery Improvement Collaborative AS (MUSIC).

**Calibration-in-the-large** We first assessed calibration-in-the-large [10]  
 of our model in the aforementioned cohorts. To this end, we used our model  
 to predict the cause-specific cumulative upgrading-risk for each patient, given  
 their PSA measurements and biopsy results. We then averaged the resulting  
 profiles of cause-specific cumulative upgrading-risk. Subsequently, we com-  
 pared the averaged cumulative-risk profile with a non-parametric estimate [7]  
 of the cause-specific cumulative upgrading-risk in each of the cohorts. The  
 results are shown in Panel A of Figure 6. We can see that our model is  
 miscalibrated in external cohorts, although it is fine in the Hopkins cohort.  
 To improve our model’s calibration in all cohorts, we recalibrated the base-  
 line hazard of the joint model fitted to the PRIAS dataset, individually for  
 each of the cohorts except the Hopkins cohort. More specifically, given the  
 data of an external cohort  $\mathcal{A}^c$ , where  $c$  denotes the cohort, the recalibrated  
 parameters  $\gamma_{h_0}^c$  (Appendix A) of the log baseline hazard are given by:

$$p(\gamma_{h_0}^c \mid \mathcal{A}^c, \mathbf{b}^c, \boldsymbol{\theta}) \propto \prod_{i=1}^{n^c} p(l_i^c, r_i^c \mid \mathbf{b}_i^c, \boldsymbol{\theta}) p(\gamma_{h_0}^c) \quad (5)$$

97 where  $n^c$  are the number of patients in the  $c$ -th cohort, and  $\boldsymbol{\theta}$  is the vector of  
 98 all parameters of the joint model fitted to the PRIAS dataset. The interval in  
 99 which upgrading is observed for the  $i$ -th patient is given by  $l_i^c, r_i^c$ , with  $r_i^c = \infty$   
 100 for right-censored patients. The symbol  $\mathbf{b}_i^c$  denotes patient-specific random  
 101 effects (Appendix A) in the  $c$ -th cohort. The random effects are obtained  
 102 using the joint model fitted to the PRIAS dataset before recalibration. We  
 103 re-evaluated the calibration-in-the-large of our model after the recalibration  
 104 of the baseline hazard individually for each cohort. The improved calibration-  
 105 in-the-large is shown in Panel B of Figure 6.

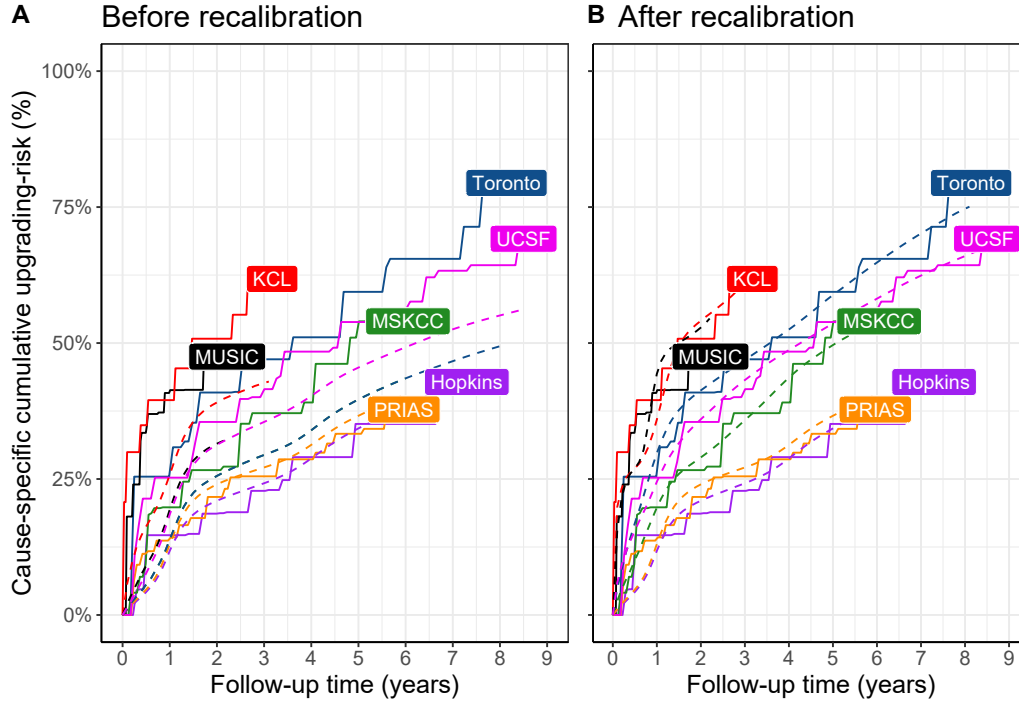


Figure 6: **Calibration-in-the-large of our model:** In **Panel A** we can see that our model is not well calibrated for use in KCL, MUSIC, Toronto and MSKCC. In **Panel B** we can see that calibration of model predictions improved in KCL, MUSIC, Toronto and MSKCC cohorts after recalibrating our model. Recalibration was not necessary for Hopkins cohort. Full names of Cohorts are *PRIAS*: Prostate Cancer International Active Surveillance, *Toronto*: University of Toronto Active Surveillance, *Hopkins*: Johns Hopkins Active Surveillance, *MSKCC*: Memorial Sloan Kettering Cancer Center Active Surveillance, *KCL*: King's College London Active Surveillance, *MUSIC*: Michigan Urological Surgery Improvement Collaborative Active Surveillance, *UCSF*: University of California San Francisco Active Surveillance.

106     ***Recalibrated PRIAS Model Versus Individual Joint Models***  
107     ***For Each Cohort*** We wanted to check if our recalibrated PRIAS model  
108 performed as good as a new joint model that could be fitted to the external  
109 cohorts. To this end, we predicted cause-specific cumulative upgrading-risk  
110 for each patient from each cohort using two sets of models, namely the recal-  
111 ibrated PRIAS model for each cohort, and a new joint model fitted to each  
112 cohort. The difference in predicted cause-specific cumulative upgrading-risk  
113 from these models is shown in Figure 7. We can see that the difference is  
114 smaller in those cohorts in which the effects of  $\log_2(\text{PSA} + 1)$  value and ve-  
115 locity were similar to that of PRIAS (Table 8). For example, the Hopkins  
116 cohort had parameter estimates similar to that of PRIAS, and consequently,  
117 the difference in predicted risks for this cohort is smallest. The opposite of  
118 this phenomenon holds for the MUSIC and KCL cohorts.



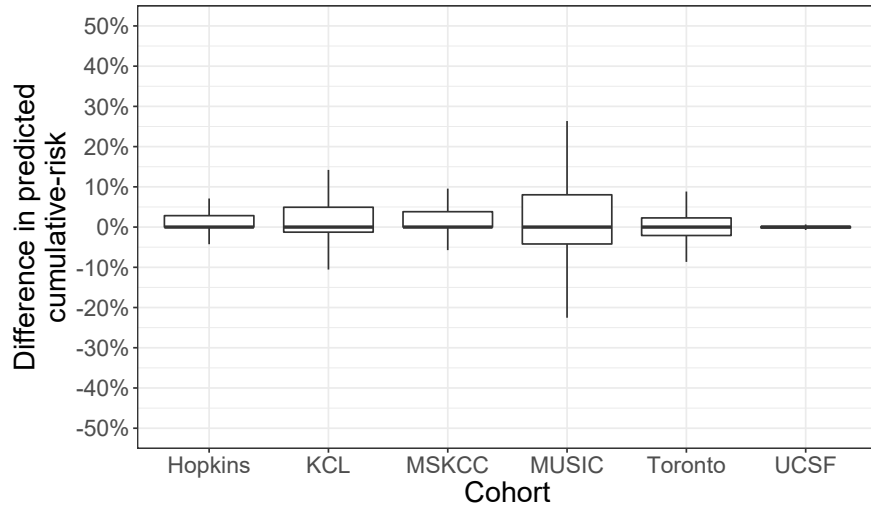


Figure 7: **Comparison of predictions from recalibrated PRIAS model with individual joint models fitted to external cohorts:** On Y-axis we show the difference between predicted cause-specific cumulative upgrading-risk for individual patients using two models, namely the recalibrated PRIAS model for each cohort, and individual joint model fitted to each cohort. The figure shows that the difference is smaller in those cohorts in which the effects of  $\log_2(\text{PSA} + 1)$  value and velocity were similar to that of PRIAS (Table 8). Full names of Cohorts are *PRIAS*: Prostate Cancer International Active Surveillance, *Toronto*: University of Toronto Active Surveillance, *Hopkins*: Johns Hopkins Active Surveillance, *MSKCC*: Memorial Sloan Kettering Cancer Center Active Surveillance, *KCL*: King’s College London Active Surveillance, *MUSIC*: Michigan Urological Surgery Improvement Collaborative Active Surveillance, *UCSF*: University of California San Francisco Active Surveillance.

**Validation of Dynamic Cumulative-Risk Predictions** As shown in Figure 5, the cumulative-risk predictions from the joint model are dynamic in nature. That is, they update as more data becomes available over time. Consequently, the discrimination and prediction error of the joint model also depend on the available data. We assessed these two measures dynamically in the PRIAS cohort (interval validation) and in the largest six external cohorts that are part of the GAP3 database. For discrimination, we utilized the time-varying area under the receiver operating characteristic curve or time-varying AUC [9]. For time-varying prediction error, we assessed the mean absolute prediction error or MAPE [9]. The AUC indicates how well the model discriminates between patients who experience upgrading, and those do not. The MAPE indicates how accurately the model predicts upgrading. Both AUC and MAPE are restricted to  $[0, 1]$ . However, it is preferred that  $\text{AUC} > 0.5$  because an  $\text{AUC} \leq 0.5$  indicates that the model performs worse than random discrimination. Ideally, MAPE should be 0.

We calculate AUC and MAPE in a time-dependent manner. More specifically, given the time of latest biopsy  $t$ , and history of PSA measurements up to time  $v$ , we calculate AUC and MAPE for a medically relevant time frame  $(t, v]$ , within which the occurrence of upgrading is of interest. In the case of prostate cancer, at any point in time  $v$ , it is of interest to identify patients who may have experienced upgrading in the last one year  $(v - 1, v]$ . That is, we set  $t = v - 1$ . We then calculate AUC and MAPE at a gap of every six months (follow-up schedule of PRIAS). That is,  $v \in \{1, 1.5, \dots\}$  years. To obtain reliable estimates of AUC and MAPE, in each cohort, we restrict  $v$  to a maximum time point  $v_{\max}$ , such that there are at least ten patients who experience upgrading after  $v_{\max}$ . This maximum time point  $v_{\max}$  differs between cohorts, and is given in Table 9.

The results for estimates of AUC and MAPE are summarized in Figure 8, and in Table 10 to Table 16. Results are based on the recalibrated PRIAS model for the GAP3 cohorts. The results show that AUC remains more or less constant in all cohorts as more data becomes available for patients. The AUC obtains a moderate value, roughly between 0.5 and 0.7 for all cohorts. On the other hand, MAPE reduces by a big margin after year one of follow-up. This could be because of two reasons. Firstly, MAPE at year one is based only on four PSA measurements gathered in the first year of follow-up, whereas after year one number of PSA measurements increases. Secondly, patients in year one consist of two sub-populations, namely patients with a correct Gleason grade group 1 at the time of inclusion in AS, and patients

Table 9: **Maximum follow-up period up to which we can reliably predict upgrading-risk.** In each cohort, this time point is chosen such that there are at least 10 patients who experience upgrading after this time point. Full names of Cohorts are *PRIAS*: Prostate Cancer International Active Surveillance, *Toronto*: University of Toronto Active Surveillance, *Hopkins*: Johns Hopkins Active Surveillance, *MSKCC*: Memorial Sloan Kettering Cancer Center Active Surveillance, *KCL*: King's College London Active Surveillance, *MUSIC*: Michigan Urological Surgery Improvement Collaborative Active Surveillance, *UCSF*: University of California San Francisco Active Surveillance.

Cohort	Maximum Prediction Time (years)
PRIAS	6
KCL	3
MUSIC	2
Toronto	8
MSKCC	6
Hopkins	7
UCSF	8.5

157 who probably had Gleason grade group 2 at inclusion but were misclassified  
 158 by the urologist as Gleason grade group 1 patients. To remedy this problem,  
 159 a biopsy for all patients at year one is commonly recommended in all AS  
 160 programs [11].

Table 10: **Internal validation of predictions of upgrading in PRIAS cohort.** The area under the receiver operating characteristic curve or AUC (measure of discrimination) and mean absolute prediction error or MAPE are calculated over the follow-up period at a gap of 6 months. In addition bootstrapped 95% confidence intervals (CI) are also presented.

Follow-up period (years)	AUC (95% CI)	MAPE (95%CI)
0.0 to 1.0	0.652 [0.611, 0.690]	0.220 [0.214, 0.227]
0.5 to 1.5	0.657 [0.641, 0.673]	0.260 [0.254, 0.265]
1.0 to 2.0	0.661 [0.647, 0.678]	0.187 [0.183, 0.191]
1.5 to 2.5	0.647 [0.596, 0.688]	0.129 [0.122, 0.140]
2.0 to 3.0	0.683 [0.642, 0.723]	0.135 [0.125, 0.146]
2.5 to 3.5	0.692 [0.632, 0.748]	0.118 [0.111, 0.128]
3.0 to 4.0	0.657 [0.603, 0.709]	0.086 [0.080, 0.092]
3.5 to 4.5	0.623 [0.582, 0.660]	0.111 [0.105, 0.116]
4.0 to 5.0	0.619 [0.582, 0.654]	0.126 [0.118, 0.131]
4.5 to 5.5	0.624 [0.537, 0.711]	0.119 [0.103, 0.135]
5.0 to 6.0	0.639 [0.582, 0.696]	0.121 [0.103, 0.138]

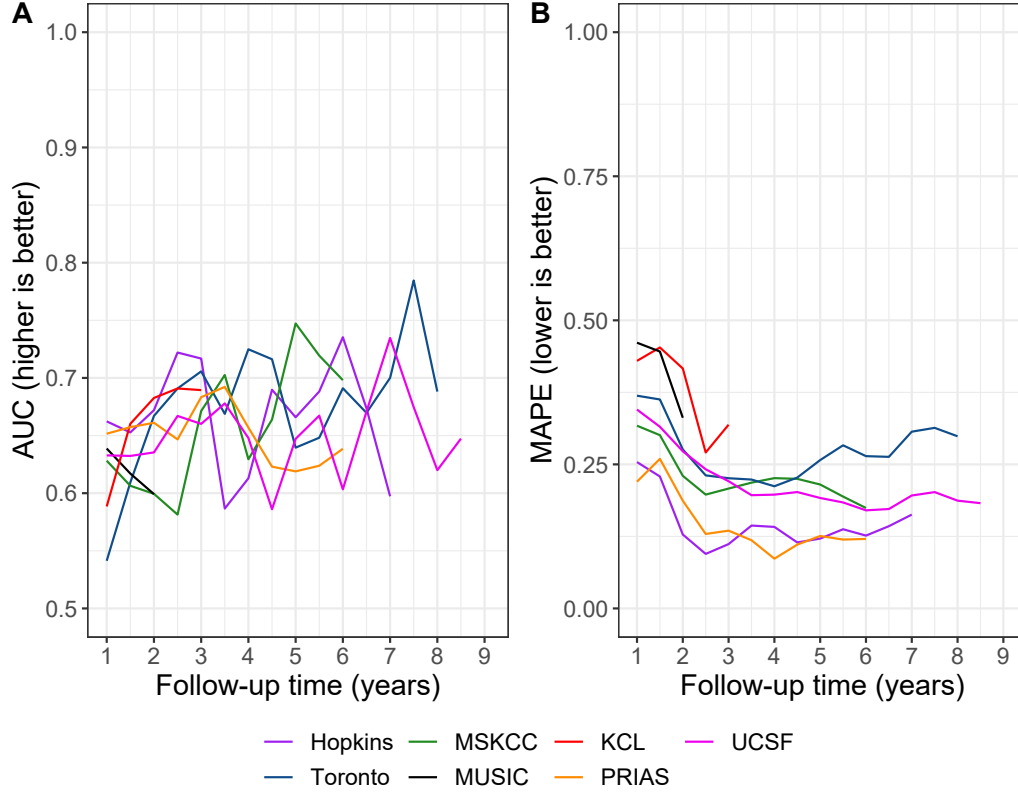


Figure 8: **Validation of dynamic predictions of cause-specific cumulative upgrading-risk.** In **Panel A** we can see that the time dependent area under the receiver operating characteristic curve or AUC (measure of discrimination) is above 0.5 in PRIAS (internal validation), and in Toronto, Hopkins, MSKCC, KCL, and MUSIC AS cohorts (external validation). In **Panel B** we can see that the time dependent root mean squared prediction error or MAPE is similar for PRIAS and Hopkins cohorts. The bootstrapped 95% confidence interval for these estimates are presented in Table 10 to Table 15. Full names of Cohorts are *PRIAS*: Prostate Cancer International Active Surveillance, *Toronto*: University of Toronto Active Surveillance, *Hopkins*: Johns Hopkins Active Surveillance, *MSKCC*: Memorial Sloan Kettering Cancer Center Active Surveillance, *KCL*: King's College London Active Surveillance, *MUSIC*: Michigan Urological Surgery Improvement Collaborative Active Surveillance, *UCSF*: University of California San Francisco Active Surveillance.

Table 11: **External validation of predictions of upgrading in University of Toronto Active Surveillance cohort.** The area under the receiver operating characteristic curve or AUC (measure of discrimination) and mean absolute prediction error or MAPE are calculated over the follow-up period at a gap of 6 months. In addition bootstrapped 95% confidence intervals (CI) are also presented.

Follow-up period (years)	AUC (95% CI)	MAPE (95%CI)
0.0 to 1.0	0.541 [0.470, 0.621]	0.369 [0.352, 0.381]
0.5 to 1.5	0.609 [0.547, 0.661]	0.363 [0.348, 0.376]
1.0 to 2.0	0.667 [0.634, 0.712]	0.276 [0.259, 0.296]
1.5 to 2.5	0.691 [0.651, 0.730]	0.231 [0.205, 0.254]
2.0 to 3.0	0.706 [0.637, 0.762]	0.226 [0.196, 0.260]
2.5 to 3.5	0.669 [0.586, 0.741]	0.224 [0.195, 0.258]
3.0 to 4.0	0.725 [0.649, 0.806]	0.212 [0.184, 0.238]
3.5 to 4.5	0.716 [0.642, 0.793]	0.227 [0.206, 0.258]
4.0 to 5.0	0.640 [0.579, 0.717]	0.257 [0.222, 0.312]
4.5 to 5.5	0.648 [0.579, 0.740]	0.283 [0.247, 0.326]
5.0 to 6.0	0.691 [0.608, 0.793]	0.264 [0.232, 0.302]
5.5 to 6.5	0.670 [0.543, 0.776]	0.263 [0.227, 0.307]
6.0 to 7.0	0.700 [0.544, 0.851]	0.307 [0.258, 0.363]
6.5 to 7.5	0.785 [0.640, 0.866]	0.313 [0.272, 0.360]
7.0 to 8.0	0.688 [0.532, 0.786]	0.299 [0.249, 0.361]

Table 12: **External validation of predictions of upgrading in University of California San Francisco Active Surveillance cohort.** The area under the receiver operating characteristic curve or AUC (measure of discrimination) and mean absolute prediction error or MAPE are calculated over the follow-up period at a gap of 6 months. In addition bootstrapped 95% confidence intervals (CI) are also presented.

Follow-up period (years)	AUC (95% CI)	MAPE (95%CI)
0.0 to 1.0	0.633 [0.585, 0.674]	0.345 [0.337, 0.357]
0.5 to 1.5	0.632 [0.599, 0.673]	0.315 [0.308, 0.323]
1.0 to 2.0	0.635 [0.595, 0.677]	0.273 [0.266, 0.281]
1.5 to 2.5	0.667 [0.628, 0.715]	0.241 [0.224, 0.259]
2.0 to 3.0	0.660 [0.600, 0.713]	0.221 [0.205, 0.238]
2.5 to 3.5	0.678 [0.614, 0.757]	0.197 [0.175, 0.214]
3.0 to 4.0	0.648 [0.574, 0.707]	0.197 [0.179, 0.221]
3.5 to 4.5	0.586 [0.525, 0.638]	0.202 [0.180, 0.229]
4.0 to 5.0	0.647 [0.590, 0.754]	0.192 [0.168, 0.217]
4.5 to 5.5	0.667 [0.582, 0.773]	0.184 [0.159, 0.220]
5.0 to 6.0	0.603 [0.496, 0.696]	0.170 [0.144, 0.207]
5.5 to 6.5	0.671 [0.576, 0.786]	0.173 [0.145, 0.202]
6.0 to 7.0	0.735 [0.663, 0.794]	0.196 [0.166, 0.219]
6.5 to 7.5	0.675 [0.565, 0.769]	0.202 [0.168, 0.231]
7.0 to 8.0	0.620 [0.518, 0.740]	0.187 [0.144, 0.217]
7.5 to 8.5	0.647 [0.538, 0.787]	0.183 [0.146, 0.222]

Table 13: **External validation of predictions of upgrading in Johns Hopkins Active Surveillance cohort.** The area under the receiver operating characteristic curve or AUC (measure of discrimination) and mean absolute prediction error or MAPE are calculated over the follow-up period at a gap of 6 months. In addition bootstrapped 95% confidence intervals (CI) are also presented.

Follow-up period (years)	AUC (95% CI)	MAPE (95%CI)
0.0 to 1.0	0.662 [0.586, 0.715]	0.254 [0.245, 0.265]
0.5 to 1.5	0.653 [0.603, 0.707]	0.229 [0.219, 0.240]
1.0 to 2.0	0.672 [0.604, 0.744]	0.128 [0.115, 0.141]
1.5 to 2.5	0.722 [0.652, 0.792]	0.095 [0.081, 0.111]
2.0 to 3.0	0.717 [0.638, 0.777]	0.112 [0.100, 0.123]
2.5 to 3.5	0.587 [0.493, 0.704]	0.144 [0.129, 0.154]
3.0 to 4.0	0.613 [0.486, 0.742]	0.141 [0.126, 0.156]
3.5 to 4.5	0.690 [0.594, 0.783]	0.115 [0.100, 0.133]
4.0 to 5.0	0.666 [0.572, 0.754]	0.121 [0.104, 0.147]
4.5 to 5.5	0.688 [0.519, 0.779]	0.137 [0.119, 0.161]
5.0 to 6.0	0.735 [0.676, 0.820]	0.126 [0.102, 0.152]
5.5 to 6.5	0.674 [0.581, 0.765]	0.143 [0.121, 0.172]
6.0 to 7.0	0.597 [0.472, 0.712]	0.163 [0.126, 0.195]

Table 14: **External validation of predictions of upgrading in Memorial Sloan Kettering Cancer Center Active Surveillance cohort.** The area under the receiver operating characteristic curve or AUC (measure of discrimination) and mean absolute prediction error or MAPE are calculated over the follow-up period at a gap of 6 months. In addition bootstrapped 95% confidence intervals (CI) are also presented.

Follow-up period (years)	AUC (95% CI)	MAPE (95%CI)
0.0 to 1.0	0.628 [0.577, 0.688]	0.317 [0.316, 0.318]
0.5 to 1.5	0.606 [0.532, 0.657]	0.301 [0.290, 0.311]
1.0 to 2.0	0.599 [0.518, 0.671]	0.230 [0.207, 0.256]
1.5 to 2.5	0.581 [0.504, 0.663]	0.198 [0.168, 0.235]
2.0 to 3.0	0.671 [0.599, 0.741]	0.208 [0.182, 0.232]
2.5 to 3.5	0.703 [0.610, 0.777]	0.218 [0.197, 0.246]
3.0 to 4.0	0.629 [0.499, 0.706]	0.226 [0.194, 0.259]
3.5 to 4.5	0.664 [0.589, 0.756]	0.225 [0.199, 0.262]
4.0 to 5.0	0.747 [0.642, 0.841]	0.215 [0.188, 0.247]
4.5 to 5.5	0.719 [0.597, 0.852]	0.194 [0.165, 0.232]
5.0 to 6.0	0.698 [0.565, 0.792]	0.174 [0.136, 0.227]

Table 15: **External validation of predictions of upgrading in King's College London Active Surveillance cohort.** The area under the receiver operating characteristic curve or AUC (measure of discrimination) and mean absolute prediction error or MAPE are calculated over the follow-up period at a gap of 6 months. In addition bootstrapped 95% confidence intervals (CI) are also presented.

Follow-up period (years)	AUC (95% CI)	MAPE (95%CI)
0.0 to 1.0	0.589 [0.514, 0.653]	0.430 [0.407, 0.450]
0.5 to 1.5	0.660 [0.550, 0.742]	0.453 [0.431, 0.474]
1.0 to 2.0	0.683 [0.604, 0.753]	0.416 [0.396, 0.445]
1.5 to 2.5	0.691 [0.621, 0.766]	0.271 [0.246, 0.297]
2.0 to 3.0	0.689 [0.616, 0.785]	0.319 [0.282, 0.344]

Table 16: **External validation of predictions of upgrading in Michigan Urological Surgery Improvement Collaborative Active Surveillance cohort.** The area under the receiver operating characteristic curve or AUC (measure of discrimination) and mean absolute prediction error or MAPE are calculated over the follow-up period at a gap of 6 months. In addition bootstrapped 95% confidence intervals (CI) are also presented.

Follow-up period (years)	AUC (95% CI)	MAPE (95%CI)
0.0 to 1.0	0.639 [0.607, 0.672]	0.461 [0.450, 0.469]
0.5 to 1.5	0.617 [0.588, 0.652]	0.446 [0.441, 0.453]
1.0 to 2.0	0.599 [0.553, 0.632]	0.331 [0.317, 0.348]



## 161 Appendix C. Personalized Biopsies Based on Cause-Specific Cu- 162 mulative Upgrading-Risk

163 Consider some real patients from the PRIAS database shown in Fig-  
164 ure 10– 12. In line with the protocols of most AS cohorts [12], we first  
165 schedule a compulsory biopsy at year one of follow-up. This promises early  
166 detection of Gleason upgrade for patients misdiagnosed as low-grade cancer  
167 patients or patients who chose AS despite having a higher grade at diagnosis.  
168 We also maintain a recommended minimum gap of one year between consec-  
169 utive biopsies [11]. That is, we intend to develop a personalized schedule of  
170 biopsies for these patients starting from the second year. The added benefit  
171 of planning biopsies year two onwards is that due to the longitudinal mea-  
172 surements accumulated over two years, and year one biopsy results, we are  
173 able to make reasonably accurate predictions of the cause-specific cumulative  
174 upgrading-risk.

Using the joint model fitted to the PRIAS dataset, we first obtain a pa-  
tient’s cause-specific cumulative upgrading-risk over the entire future follow-  
up period (see 4), given their accumulated two year clinical data. Typically  
biopsies may be decided on the same visit on which PSA is measured. Let  
 $U = u_1, \dots, u_L$  represent a schedule of such visits (e.g., every six months in  
prostate cancer for PSA measurement), where  $u_1 = v$  is also the time of the  
current visit, and  $u_L$  is the horizon up to which we intend to plan biopsies.  
Depending upon how much training/validation data is available, this horizon  
differs between cohorts (Table 17). First, we make  $L$  successive decisions for  
conducting biopsies on each of the  $L$  future visit times  $u_l \in U$ . Specifically,  
we decide to conduct a biopsy at time  $u_l$  if the conditional cumulative-risk  
of upgrading at  $u_l$  is larger than a certain risk threshold  $0 \leq \kappa \leq 1$  (e.g.,  
 $\kappa = 12\%$  risk as shown in Figure 9). If a biopsy gets planned at time  $u_l$ ,  
then the successive biopsy decision at time  $u_{l+1}$  is made using an updated  
cumulative-risk profile. This updated cumulative-risk profile accounts for  
the possibility that upgrading may occur after time  $u_l < T_j^*$ . The biopsy  
decisions on each future visit time  $u_l$  are defined as:

$$Q_j^\kappa(u_l | t_l, v) = I\{R_j(u_l | t_l, v) \geq \kappa\},$$

$$t_l = \begin{cases} t, & \text{if } l = 1 \\ t_{l-1}, & \text{if } Q_j^\kappa(u_{l-1} | t_{l-1}, v) = 0, l \geq 2 \\ u_{l-1}, & \text{if } Q_j^\kappa(u_{l-1} | t_{l-1}, v) = 1, l \geq 2 \end{cases}.$$

The cumulative-risk  $R_j(u_l | t_l, v)$  at future visit time  $u_l$  utilizes the time  $t_l$

as the time of the last conducted biopsy on which upgrading may not be observed. However, the contribution of the observed longitudinal data  $\mathcal{Y}_j(v)$  in the risk function remains the same over all time points in  $U$ . The biopsy decision at time  $u_l$  is denoted by  $Q_j^\kappa(u_l | t_l, v)$ . Via the indicator function  $I(\cdot)$  it obtains a value 1 (or 0) when a biopsy is to be conducted (or not conducted) at time  $u_l$ . The subset of future time points in  $U$  on which a biopsy is to be performed results into a personalized schedule of planned future biopsies, given by:

$$S_j^\kappa(U | t, v) = \{u_l \in U | Q_j^\kappa(u_l | t_l, v) = 1\}. \quad (6)$$

175 The personalized schedule in (6) is updated as more patient data becomes  
176 available over subsequent follow-up visits.

#### 177 *Appendix C.1. Expected Time Delay in Detecting Upgrading*

178 The schedule  $S_j^\kappa(U | t, v)$  manifests a personalized biopsy plan for the  
179  $j$ -the patient. However, the time delay in detecting upgrading that may  
180 subsequently be observed depends on the true time of upgrading  $T_j^*$  of the  
181 patient. Since two different patients with the same timing of biopsies will  
182 expect different time delays, we estimate it in a patient-specific manner as  
183 well. Although, this calculation is not limited to personalized schedules only,  
184 but can be done for any schedule  $S$  of biopsies with  $N$  time points  $S = \{s_n |$   
185  $n = 1, \dots, N\}$ .

For each of the  $N$  planned biopsies there exist  $N$  possible time intervals  $s_{n-1} < T_j^* \leq s_n$  in which upgrading may be observed. Correspondingly, there are  $N$  possible time delays in detecting upgrading  $s_n - T_j^*$ . Given a schedule  $S$ , the true time delay in detecting upgrading  $D_j$  that the patient will experience can be defined as:

$$D_j(S | t) = \left\{ \begin{array}{ll} s_1 - T_j^*, & \text{if } t < T_j^* \leq s_1 \\ \dots & \\ s_N - T_j^*, & \text{if } s_{N-1} < T_j^* \leq s_N \end{array} \right\}. \quad (7)$$

The time delay is cannot be defined for the scenario in which the patient obtains upgrading after the time of the last biopsy in the schedule  $T_j^* > s_N$ . Hence, this delay should be interpreted as the delay that will be observed if the patient will experience upgrading before time of the last planned biopsy at  $T_j^* \leq s_N$ . To estimate the expected value of  $D_j(\cdot)$  in a patient-specific manner, we exploit the personalized cumulative-risk profile of the patient

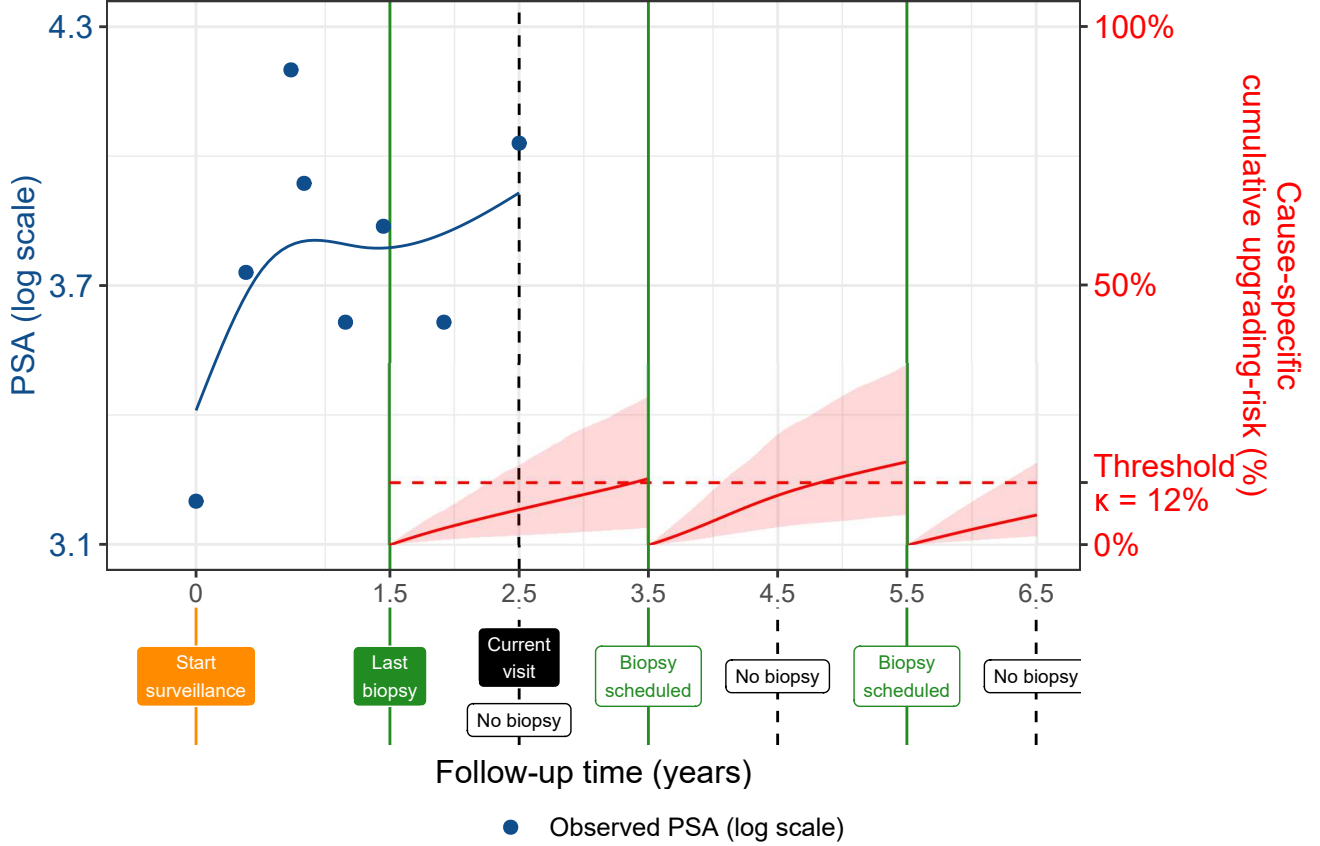


Figure 9: **Illustration of Personalized Biopsy Decisions Using Patient-specific Conditional Cumulative Upgrading-risk.** The last biopsy on which upgrading was not observed was conducted at  $t = 1.5$  years. The current visit time of the patient is  $v = 2.5$  years. Decisions for biopsy need to be made at a gap of every one year starting from the current visit until a horizon of 6.5 years. That is,  $U = \{2.5, 3.5, 4.5, 5.5, 6.5\}$  years. Based on an example risk threshold of 12% ( $\kappa = 0.12$ ) the future biopsy decisions at time points in  $U$  lead to a personalized schedule  $S_j^{\kappa^*}(U \mid t = 1.5, v = 2.5) = \{3.5, 5.5\}$  years. The conditional cumulative-risk profiles  $R_j(u_l \mid t_l, v)$  employed in (Appendix C) are shown with red line (confidence interval shaded). It is called ‘conditional’ because, for example, the second biopsy at future time 5.5 years, is scheduled after accounting for the possibility that upgrading (true time  $T_j^*$ ) may not have occurred until the time of the previously scheduled biopsy at time  $T_j^* > 3.5$  years. All values are illustrative.

defined in (4). Specifically, the expected time delay  $E\{D_j(\cdot)\}$  can be calculated as the weighted sum of  $N$  possible time delays defined in (7). The  $n$ -th weight is equal to the probability of the patient obtaining upgrading in the  $n$ -th interval  $s_{n-1} < T_j^* \leq s_n$ .

$$\begin{aligned}
 E\{D_j(S | t)\} &= \sum_{n=1}^N \left\{ s_n - E(T_j^* | s_{n-1}, s_n, v) \right\} \\
 &\quad \times \Pr\left\{ s_{n-1} < T_j^* \leq s_n \mid T_j^* \leq s_N, \mathcal{Y}_j(v), \mathcal{A}_n \right\}, \quad s_0 = t \\
 E(T_j^* | s_{n-1}, s_n, v) &= s_{n-1} + \int_{s_{n-1}}^{s_n} \Pr\left\{ T_j^* \geq u \mid s_{n-1} < T_j^* \leq s_n, \mathcal{Y}_j(v), \mathcal{A}_n \right\} du,
 \end{aligned}$$

186 where  $E(T_j^* | s_{n-1}, s_n, v)$  denotes the conditional expected time of upgrading  
 187 for the scenario  $s_{n-1} < T_j^* \leq s_n$ , and is calculated as the area under the  
 188 corresponding survival curve.

189 The personalized expected time delay in detecting upgrading has the  
 190 advantage that it is updated over follow-up as more patient data become  
 191 available. Since it can be calculated for any schedule, patients and doctors  
 192 can utilize it along with the plan of biopsies to compare schedules before  
 193 making a decision. Although, in order to have a fair comparison of time  
 194 delays between different schedules for the same patient, a compulsory biopsy  
 195 at a common horizon time point should be planned in all schedules.

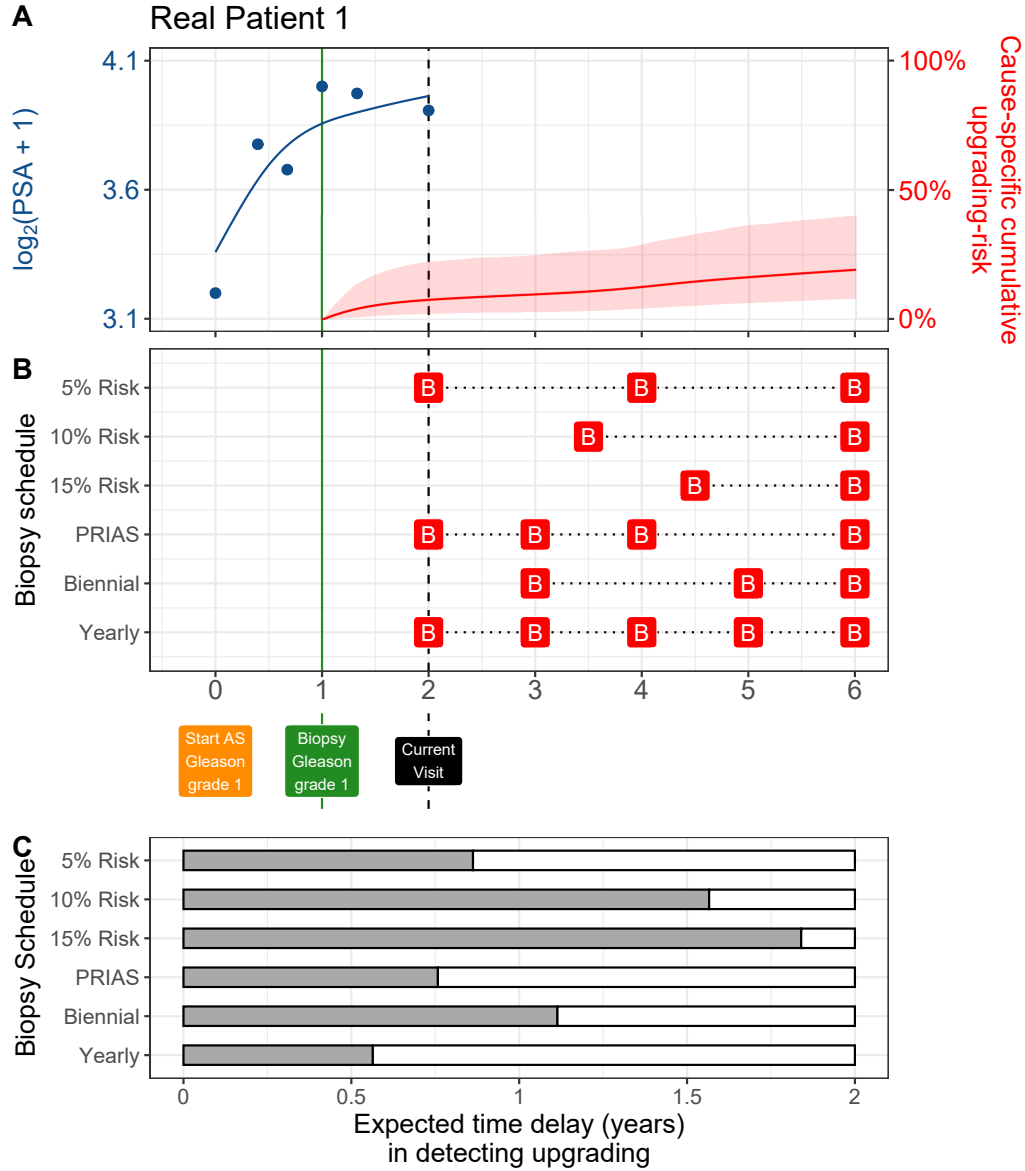


Figure 10: **Personalized and fixed schedules of biopsies for patient 1.** **Panel A:** shows the observed and fitted  $\log_2(\text{PSA} + 1)$  measurements (Equation 1), and the dynamic cause-specific cumulative upgrading-risk (see Appendix B) over follow-up period. **Panel B** shows the personalized and fixed schedules of biopsies with a 'B' indicating times of biopsies. **Panel C** various schedules are compared in terms of the expected time delay in detecting upgrading (years) if patient progresses before year six. A compulsory biopsy was scheduled at year six (maximum biopsy scheduling time in PRIAS, Table 17) in all schedules for a meaningful comparison between them.

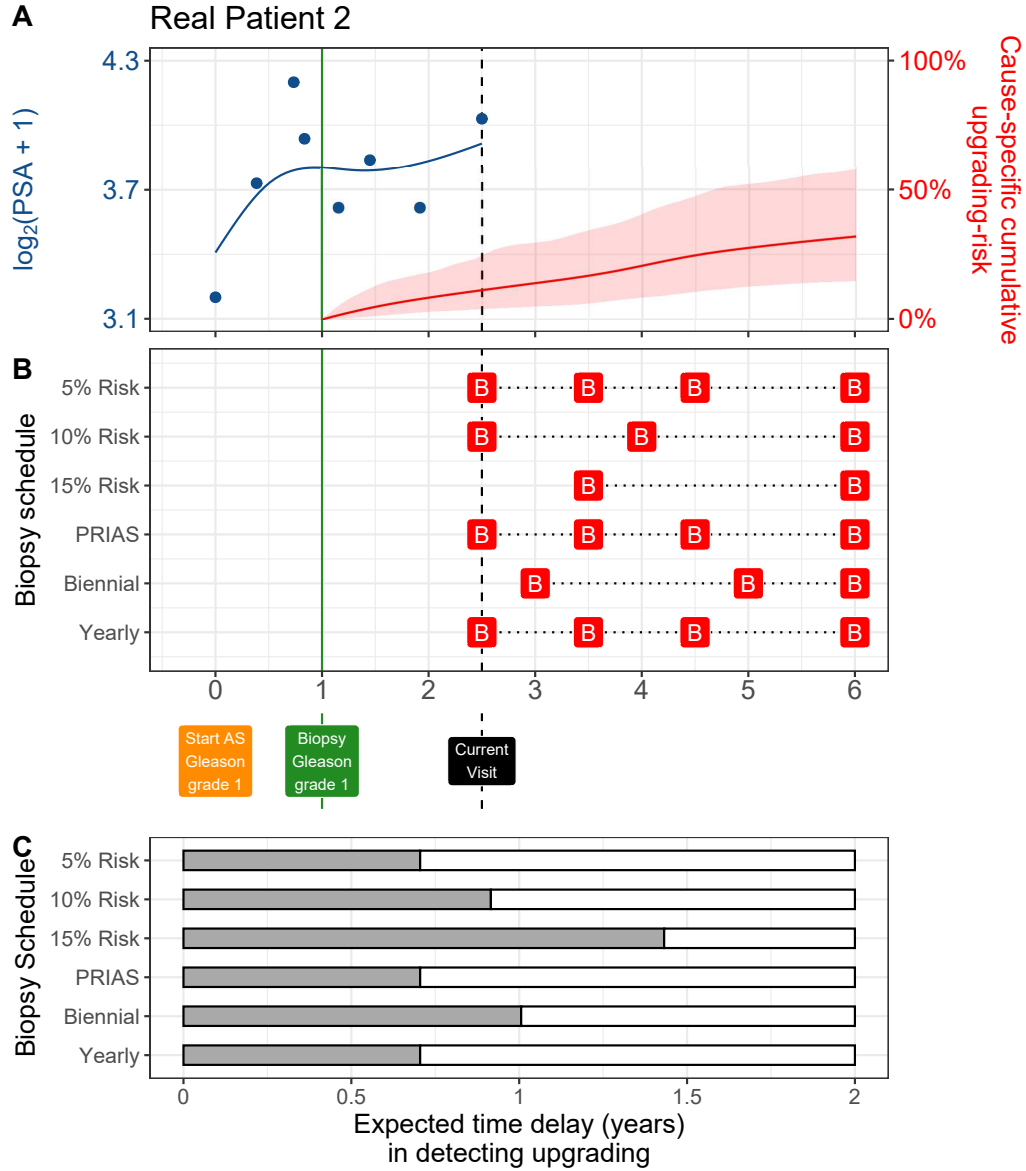


Figure 11: **Personalized and fixed schedules of biopsies for patient 2.** **Panel A:** shows the observed and fitted  $\log_2(\text{PSA} + 1)$  measurements (Equation 1), and the dynamic cause-specific cumulative upgrading-risk (see Appendix B) over follow-up period. **Panel B** shows the personalized and fixed schedules of biopsies with a 'B' indicating times of biopsies. **Panel C** various schedules are compared in terms of the expected time delay in detecting upgrading (years) if patient progresses before year six. A compulsory biopsy was scheduled at year six (maximum biopsy scheduling time in PRIAS, Table 17) in all schedules for a meaningful comparison between them.

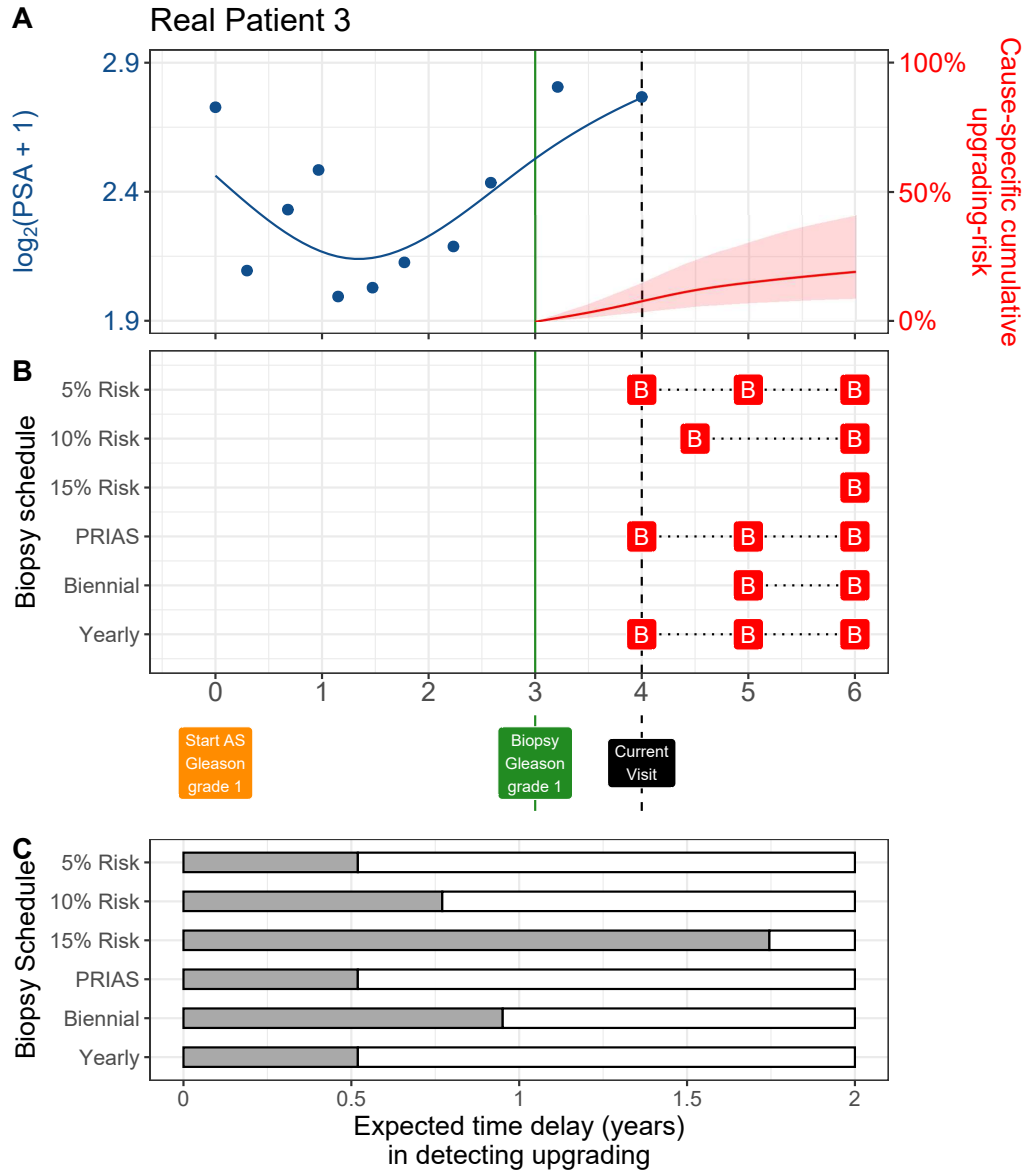


Figure 12: **Personalized and fixed schedules of biopsies for patient 3.** **Panel A:** shows the observed and fitted  $\log_2(\text{PSA} + 1)$  measurements (Equation 1), and the dynamic cause-specific cumulative upgrading-risk (see Appendix B) over follow-up period. **Panel B** shows the personalized and fixed schedules of biopsies with a 'B' indicating times of biopsies. **Panel C** various schedules are compared in terms of the expected time delay in detecting upgrading (years) if patient progresses before year six. A compulsory biopsy was scheduled at year six (maximum biopsy scheduling time in PRIAS, Table 17) in all schedules for a meaningful comparison between them.

Table 17: **Maximum follow-up period up to which we can reliably make personalized schedules.** In each cohort, this time point is chosen such that there are at least 10 patients who experience upgrading after this time point. Full names of Cohorts are *PRIAS*: Prostate Cancer International Active Surveillance, *Toronto*: University of Toronto Active Surveillance, *Hopkins*: Johns Hopkins Active Surveillance, *MSKCC*: Memorial Sloan Kettering Cancer Center Active Surveillance, *KCL*: King's College London Active Surveillance, *MUSIC*: Michigan Urological Surgery Improvement Collaborative Active Surveillance, *UCSF*: University of California San Francisco Active Surveillance.

Cohort	Maximum Personalized Schedule Time (years)
PRIAS	6
KCL	3
MUSIC	2
Toronto	8
MSKCC	6
Hopkins	7
UCSF	8.5



## Appendix D. Web-Application for Practical Use of Personalized Schedule of Biopsies

We implemented our methodology in a web-application to assist patients and doctors in better decision making. It works on desktop as well as mobile devices. The cohorts that are currently supported in this web-application are PRIAS and the largest six cohorts from the GAP3 database [6]. These are the University of Toronto AS (Toronto), Johns Hopkins AS (Hopkins), Memorial Sloan Kettering Cancer Center AS (MSKCC), King's College London AS (KCL), Michigan Urological Surgery Improvement Collaborative AS (MUSIC), and University of California San Francisco Active Surveillance (UCSF). The web application is hosted at [https://emcbiostatistics.shinyapps.io/prias\\_biopsy\\_recommender/](https://emcbiostatistics.shinyapps.io/prias_biopsy_recommender/).

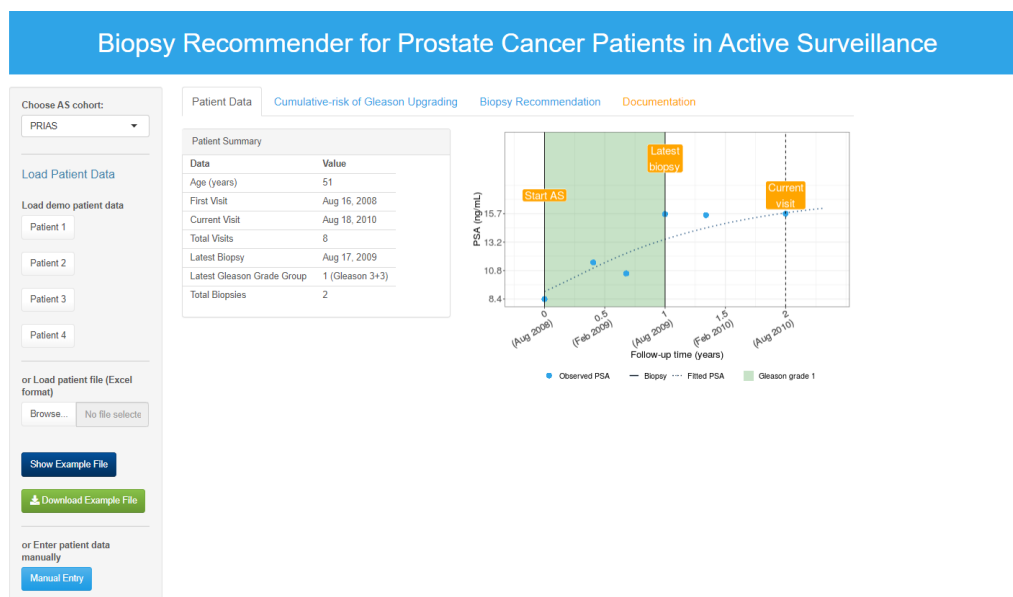


Figure 13: Landing page of the web-application. Panel on the left allows users to load patient data and panel on the right provides information. Patient data can be entered manually, or via Excel files. In addition, demo patient data is already uploaded to assist users in understanding the web-application.

## 208 Appendix E. Source Code

209 The R code for fitting the joint model to the PRIAS dataset, is at [https:](https://github.com/anirudhtomer/prias/tree/master/src/clinical_gap3)  
 210 [//github.com/anirudhtomer/prias/tree/master/src/clinical\\_gap3](https://github.com/anirudhtomer/prias/tree/master/src/clinical_gap3). We  
 211 refer to this location as ‘R\_HOME’ in the rest of this document.

### 212 *Appendix E.1. Fitting the Joint Model to the PRIAS dataset*

213 **Accessing the dataset:** The PRIAS dataset is not openly accessible.  
 214 However, access to the database can be requested via the contact links at  
 215 <https://www.prias-project.org>.

216  
 217 **Formatting the dataset:** This dataset, however, is in the so-called wide  
 218 format and also requires the removal of incorrect entries. This can be done  
 219 via the R script `R_HOME/dataset_cleaning.R`. This will lead to two R ob-  
 220 jects, namely ‘`prias_final.id`’ and ‘`prias_long_final`’. The ‘`prias_final.id`’ object  
 221 contains information about the time of upgrading for PRIAS patients. The  
 222 ‘`prias_long_final`’ object contains longitudinal PSA measurements, the time  
 223 of biopsies and results of biopsies.

224  
 225 **Fitting the joint model:** We use a joint model for time-to-event and  
 226 longitudinal data to model the evolution of PSA measurements over time,  
 227 and to simultaneously model their association with the risk of upgrading.  
 228 The R package we use for this purpose is called **JMbayes** ([https://cran.r-](https://cran.r-project.org/web/packages/JMbayes/JMbayes.pdf)  
 229 [project.org/web/packages/JMbayes/JMbayes.pdf](https://cran.r-project.org/web/packages/JMbayes/JMbayes.pdf)). The API we use, how-  
 230 ever, is currently not hosted on CRAN, and can be found here: [https:](https://github.com/anirudhtomer/JMbayes)  
 231 [//github.com/anirudhtomer/JMbayes](https://github.com/anirudhtomer/JMbayes). The joint model can be fitted via  
 232 the script `R_HOME/analysis.R`. It takes roughly 6 hours to run on an Intel  
 233 Core-i5 machine with four cores and 8GB of RAM.

234 The graphs presented in the main manuscript, and the supplementary  
 235 material can be generated by the scripts in `R_HOME/plots/`.

### 236 *Appendix E.2. Validation of Predictions of Upgrading*

237 Validations can be done using the scripts `R_HOME/validation/auc_brier/`  
 238 `auc_calculator.R`, and `R_HOME/validation/auc_brier/gof_calculator.`  
 239 `R`. For external validation access to GAP3 database is required.

240 *Appendix E.3. Creating Personalized Schedules of Biopsies*

241     Once a joint model is fitted to the PRIAS dataset, personalized schedules  
242 of biopsies based on the risk of upgrading for new patients can be developed as  
243 shown in the script `R_HOME/plots/demo_schedule_supplementary.R` or di-  
244 rectly using the script `https://raw.githubusercontent.com/anirudhtomer/`  
245 `prias/master/src/lastpaper/pers\_schedule\_api.R`.

246 *Appendix E.4. Source Code for Web Application*

247     Source code for the shiny web application which provides biopsy schedules  
248 for patients can be found at `R_HOME/shinyapp`

249 **Appendix F. Appendix A. Members of The Movember Founda-**  
 250 **tion’s Global Action Plan Prostate Cancer Active**  
 251 **Surveillance (GAP3) consortium**

252 *Principle Investigators:* Bruce Trock (Johns Hopkins University, The  
 253 James Buchanan Brady Urological Institute, Baltimore, USA), Behfar Ehdaie  
 254 (Memorial Sloan Kettering Cancer Center, New York, USA), Peter Car-  
 255 roll (University of California San Francisco, San Francisco, USA), Christo-  
 256 pher Filson (Emory University School of Medicine, Winship Cancer Insti-  
 257 tute, Atlanta, USA), Jeri Kim / Christopher Logothetis (MD Anderson  
 258 Cancer Centre, Houston, USA), Todd Morgan (University of Michigan and  
 259 Michigan Urological Surgery Improvement Collaborative (MUSIC), Michi-  
 260 gan, USA), Laurence Klotz (University of Toronto, Sunnybrook Health Sci-  
 261 ences Centre, Toronto, Ontario, Canada), Tom Pickles (University of British  
 262 Columbia, BC Cancer Agency, Vancouver, Canada), Eric Hyndman (Uni-  
 263 versity of Calgary, Southern Alberta Institute of Urology, Calgary, Canada),  
 264 Caroline Moore (University College London & University College London  
 265 Hospital Trust, London, UK), Vincent Gnanapragasam (University of Cam-  
 266 bridge & Cambridge University Hospitals NHS Foundation Trust, Cam-  
 267 bridge, UK), Mieke Van Hemelrijck (King’s College London, London, UK  
 268 & Guys and St Thomas NHS Foundation Trust, London, UK), Prokar Das-  
 269 gupta (Guys and St Thomas NHS Foundation Trust, London, UK), Chris  
 270 Bangma (Erasmus Medical Center, Rotterdam, The Netherlands/ represen-  
 271 tative of Prostate cancer Research International Active Surveillance (PRIAS)  
 272 consortium), Monique Roobol (Erasmus Medical Center, Rotterdam, The  
 273 Netherlands/ representative of Prostate cancer Research International Active  
 274 Surveillance (PRIAS) consortium), Arnauld Villers (Lille University Hospi-  
 275 tal Center, Lille, France), Antti Rannikko (Helsinki University and Helsinki  
 276 University Hospital, Helsinki, Finland), Riccardo Valdagni (Department of  
 277 Oncology and Hemato-oncology, Universit degli Studi di Milano, Radia-  
 278 tion Oncology 1 and Prostate Cancer Program, Fondazione IRCCS Istituto  
 279 Nazionale dei Tumori, Milan, Italy), Antoinette Perry (University College  
 280 Dublin, Dublin, Ireland), Jonas Hugosson (Sahlgrenska University Hospital,  
 281 Gteborg, Sweden), Jose Rubio-Briones (Instituto Valenciano de Oncologa,  
 282 Valencia, Spain), Anders Bjartell (Skne University Hospital, Malm, Swe-  
 283 den), Lukas Hefermehl (Kantonsspital Baden, Baden, Switzerland), Lee Lui  
 284 Shiong (Singapore General Hospital, Singapore, Singapore), Mark Fryden-  
 285 berg (Monash Health; Monash University, Melbourne, Australia), Yoshiyuki

286 Kakehi / Mikio Sugimoto (Kagawa University Faculty of Medicine, Kagawa,  
287 Japan), Byung Ha Chung (Gangnam Severance Hospital, Yonsei University  
288 Health System, Seoul, Republic of Korea)

289 *Pathologist:* Theo van der Kwast (Princess Margaret Cancer Centre,  
290 Toronto, Canada). Technology Research Partners: Henk Obbink (Royal  
291 Philips, Eindhoven, the Netherlands), Wim van der Linden (Royal Philips,  
292 Eindhoven, the Netherlands), Tim Hulsen (Royal Philips, Eindhoven, the  
293 Netherlands), Cees de Jonge (Royal Philips, Eindhoven, the Netherlands).

294 *Advisory Regional statisticians:* Mike Kattan (Cleveland Clinic, Cleve-  
295 land, Ohio, USA), Ji Xinge (Cleveland Clinic, Cleveland, Ohio, USA), Ken-  
296 neth Muir (University of Manchester, Manchester, UK), Artitaya Lophatananon  
297 (University of Manchester, Manchester, UK), Michael Fahey (Epworth Health-  
298 Care, Melbourne, Australia), Ewout Steyerberg (Erasmus Medical Center,  
299 Rotterdam, The Netherlands), Daan Nieboer (Erasmus Medical Center, Rot-  
300 terdam, The Netherlands); Liying Zhang (University of Toronto, Sunnybrook  
301 Health Sciences Centre, Toronto, Ontario, Canada)

302 *Executive Regional statisticians:* Ewout Steyerberg (Erasmus Medical  
303 Center, Rotterdam, The Netherlands), Daan Nieboer (Erasmus Medical Cen-  
304 ter, Rotterdam, The Netherlands); Kerri Beckmann (King's College London,  
305 London, UK & Guys and St Thomas NHS Foundation Trust, London, UK),  
306 Brian Denton (University of Michigan, Michigan, USA), Andrew Hayen (Uni-  
307 versity of Technology Sydney, Australia), Paul Boutros (Ontario Institute of  
308 Cancer Research, Toronto, Ontario, Canada).

309 *Clinical Research Partners IT Experts:* Wei Guo (Johns Hopkins Uni-  
310 versity, The James Buchanan Brady Urological Institute, Baltimore, USA),  
311 Nicole Benfante (Memorial Sloan Kettering Cancer Center, New York, USA),  
312 Janet Cowan (University of California San Francisco, San Francisco, USA),  
313 Dattatraya Patil (Emory University School of Medicine, Winship Cancer In-  
314 stitute, Atlanta, USA), Emily Tolosa (MD Anderson Cancer Centre, Hous-  
315 ton, Texas, USA), Tae-Kyung Kim (University of Michigan and Michigan  
316 Urological Surgery Improvement Collaborative, Ann Arbor, Michigan, USA),  
317 Alexandre Mamedov (University of Toronto, Sunnybrook Health Sciences  
318 Centre, Toronto, Ontario, Canada), Vincent LaPointe (University of British  
319 Columbia, BC Cancer Agency, Vancouver, Canada), Trafford Crump (Uni-  
320 versity of Calgary, Southern Alberta Institute of Urology, Calgary, Canada),  
321 Vasilis Stavrinos (University College London & University College Lon-  
322 don Hospital Trust, London, UK), Jenna Kimberly-Duffell (University of  
323 Cambridge & Cambridge University Hospitals NHS Foundation Trust, Cam-

bridge, UK), Aida Santaolalla (King's College London, London, UK & Guys  
and St Thomas NHS Foundation Trust, London, UK), Daan Nieboer (Eras-  
mus Medical Center, Rotterdam, The Netherlands), Jonathan Olivier (Lille  
University Hospital Center, Lille, France), Tiziana Rancati (Fondazione IR-  
CCS Istituto Nazionale dei Tumori di Milano, Milan, Italy), Heln Ahlgren  
(Sahlgrenska University Hospital, Gteborg, Sweden), Juanma Mascars (Insti-  
tuto Valenciano de Oncologa, Valencia, Spain), Annica Lfgren (Skne Univer-  
sity Hospital, Malm, Sweden), Kurt Lehmann (Kantonsspital Baden, Baden,  
Switzerland), Catherine Han Lin (Monash University and Epworth Health-  
Care, Melbourne, Australia), Hiromi Hiram (Kagawa University, Kagawa,  
Japan), Kwang Suk Lee (Yonsei University College of Medicine, Gangnam  
Severance Hospital, Seoul, Korea).

*Research Advisory Committee:* Guido Jenster (Erasmus MC, Rotterdam,  
the Netherlands), Anssi Auvinen (University of Tampere, Tampere, Finland),  
Anders Bjartell (Skne University Hospital, Malm, Sweden), Masoom Haider  
(University of Toronto, Toronto, Canada), Kees van Bochove (The Hyve  
B.V. Utrecht, Utrecht, the Netherlands), Ballentine Carter (Johns Hopkins  
University, Baltimore, USA until 2018).

*Management team:* Sam Gledhill (Movember Foundation, Melbourne,  
Australia), Mark Buzza / Michelle Kouspou (Movember Foundation, Mel-  
bourne, Australia), Chris Bangma (Erasmus Medical Center, Rotterdam,  
The Netherlands), Monique Roobol (Erasmus Medical Center, Rotterdam,  
The Netherlands), Sophie Bruinsma / Jozien Helleman (Erasmus Medical  
Center, Rotterdam, The Netherlands).

## References

1. Epstein JI, Egevad L, Amin MB, Delahunt B, Srigley JR, Humphrey PA.  
The 2014 international society of urological pathology (isup) consensus  
conference on gleason grading of prostatic carcinoma. *The American  
journal of surgical pathology* 2016;40(2):244–52.
2. Pearson JD, Morrell CH, Landis PK, Carter HB, Brant LJ. Mixed-  
effects regression models for studying the natural history of prostate  
disease. *Statistics in Medicine* 1994;13(5-7):587–601.
3. Lin H, McCulloch CE, Turnbull BW, Slate EH, Clark LC. A latent  
class mixed model for analysing biomarker trajectories with irregularly  
scheduled observations. *Statistics in Medicine* 2000;19(10):1303–18.

- 359 4. De Boor C. A practical guide to splines; vol. 27. Springer-Verlag New  
360 York; 1978.
- 361 5. Eilers PH, Marx BD. Flexible smoothing with B-splines and penalties.  
362 *Statistical Science* 1996;11(2):89–121.
- 363 6. Bruinsma SM, Zhang L, Roobol MJ, Bangma CH, Steyerberg EW,  
364 Nieboer D, Van Hemelrijck M, consortium MFGAPPCASG, Trock B,  
365 Ehdaie B, et al. The movember foundation’s gap3 cohort: a profile of  
366 the largest global prostate cancer active surveillance database to date.  
367 *BJU international* 2018;121(5):737–44.
- 368 7. Turnbull BW. The empirical distribution function with arbitrarily  
369 grouped, censored and truncated data. *Journal of the Royal Statisti-*  
370 *cal Society Series B (Methodological)* 1976;38(3):290–5.
- 371 8. Rizopoulos D. The R package JMbayes for fitting joint models for lon-  
372 gitudinal and time-to-event data using MCMC. *Journal of Statistical*  
373 *Software* 2016;72(7):1–46.
- 374 9. Rizopoulos D, Molenberghs G, Lesaffre EM. Dynamic predictions with  
375 time-dependent covariates in survival analysis using joint modeling and  
376 landmarking. *Biometrical Journal* 2017;59(6):1261–76.
- 377 10. Steyerberg EW, Vickers AJ, Cook NR, Gerds T, Gonen M, Obuchowski  
378 N, Pencina MJ, Kattan MW. Assessing the performance of prediction  
379 models: a framework for some traditional and novel measures. *Epidemi-*  
380 *ology (Cambridge, Mass)* 2010;21(1):128.
- 381 11. Bokhorst LP, Alberts AR, Rannikko A, Valdagni R, Pickles T, Kakehi Y,  
382 Bangma CH, Roobol MJ, PRIAS study group . Compliance rates with  
383 the Prostate Cancer Research International Active Surveillance (PRIAS)  
384 protocol and disease reclassification in noncompliers. *European Urology*  
385 2015;68(5):814–21.
- 386 12. Nieboer D, Tomer A, Rizopoulos D, Roobol MJ, Steyerberg EW. Active  
387 surveillance: a review of risk-based, dynamic monitoring. *Translational*  
388 *andrology and urology* 2018;7(1):106–15.





**EUROPEAN UROLOGY** Authorship Responsibility, Financial Disclosure, and Acknowledgment form.

By completing and signing this form, the corresponding author acknowledges and accepts full responsibility on behalf of all contributing authors, if any, regarding the statements on Authorship Responsibility, Financial Disclosure and Funding Support. Any box or line left empty will result in an incomplete submission and the manuscript will be returned to the author immediately.

Title Mr.

First Name Anirudh

Middle Name

Last Name Tomer

Degree MSc (Ph.D., M.D., Jr., etc.)

Primary Phone +31 10 70 43393 (including country code)

Fax Number (including country code)

E-mail Address a.tomer@erasmusmc.nl

**Authorship Responsibility**

By signing this form and clicking the appropriate boxes, the corresponding author certifies that each author has met all criteria below (A, B, C, and D) and hereunder indicates each author's general and specific contributions by listing his or her name next to the relevant section.

☒ A. This corresponding author certifies that:

- the manuscript represents original and valid work and that neither this manuscript nor one with substantially similar content under my authorship has been published or is being considered for publication elsewhere, except as described in an attachment, and copies of closely related manuscripts are provided; and
- if requested, this corresponding author will provide the data or will cooperate fully in obtaining and providing the data on which the manuscript is based for examination by the editors or their assignees;
- every author has agreed to allow the corresponding author to serve as the primary correspondent with the editorial office, to review the edited typescript and proof.

☒ B. Each author has given final approval of the submitted manuscript.

☒ C. Each author has participated sufficiently in the work to take public responsibility for all of the content.

☒ D. Each author qualifies for authorship by listing his or her name on the appropriate line of the categories of contributions listed below.

The authors listed below have made substantial contributions to the intellectual content of the paper in the various sections described below.

(list appropriate author next to each section – each author must be listed in at least 1 field. More than 1 author can be listed in each field.)

_ conception and design	Tomer, Nieboer, Roobol, Bjartell, and Rizopoulos
_ acquisition of data	Tomer, Nieboer, and Roobol
_ analysis and interpretation of data	Tomer, Nieboer, and Rizopoulos
_ drafting of the manuscript	Tomer, and Rizopoulos
_ critical revision of the manuscript for important intellectual content	Tomer, Nieboer, Roobol, Bjartell, Steyerberg, Rizopoulos
_ statistical analysis	Tomer, Nieboer, Steyerberg, and Rizopoulos
_ obtaining funding	Roobol, Steyerberg, and Rizopoulos
_ administrative, technical, or material support	Nieboer
_ supervision	Roobol, and Rizopoulos
_ other (specify)	none

### Financial Disclosure

☒ None of the contributing authors have any conflicts of interest, including specific financial interests and relationships and affiliations relevant to the subject matter or materials discussed in the manuscript.

OR

☐ I certify that all conflicts of interest, including specific financial interests and relationships and affiliations relevant to the subject matter or materials discussed in the manuscript (eg,

employment/ affiliation, grants or funding, consultancies, honoraria, stock ownership or options, expert testimony, royalties, or patents filed, received, or pending), are the following: (please list all conflict of interest with the relevant author's name):

### **Funding Support and Role of the Sponsor**

☒ I certify that all funding, other financial support, and material support for this research and/or work are clearly identified in the manuscript.

The name of the organization or organizations which had a role in sponsoring the data and material in the study are also listed below:

Movember Foundation's Global Action Plan Prostate Cancer Active Surveillance (GAP3) consortium

All funding or other financial support, and material support for this research and/or work, if any, are clearly identified hereunder:

The specific role of the funding organization or sponsor is as follows:

- ☐ Design and conduct of the study
- ☒ Collection of the data
- ☒ Management of the data
- ☐ Analysis
- ☐ Interpretation of the data
- ☐ Preparation
- ☐ Review
- ☐ Approval of the manuscript

OR

☐ No funding or other financial support was received.

## Acknowledgment Statement

This corresponding author certifies that:

- all persons who have made substantial contributions to the work reported in this manuscript (eg, data collection, analysis, or writing or editing assistance) but who do not fulfill the authorship criteria are named with their specific contributions in an Acknowledgment in the manuscript.
- all persons named in the Acknowledgment have provided written permission to be named.
- if an Acknowledgment section is not included, no other persons have made substantial contributions to this manuscript.

I agree with all statements above

After completing all the required fields above, this form must be uploaded with the manuscript and other required fields at the time of electronic submission.

Personalized prostate biopsies are a novel alternative to fixed one-size-fits-all schedules. The underlying statistical models are made available through a user-friendly web-application and may help to reduce unnecessary prostate biopsies while maintaining cancer control.